THE ARGO-OXYGEN PROGRAM

A white paper to promote the addition of oxygen sensors to the international Argo float program

Prepared by

Nicolas Gruber[1] (chair), Scott C. Doney[2], Steven R. Emerson[3], Denis Gilbert[4], Taiyo Kobayashi[5], Arne Körtzinger[6], Gregory C. Johnson[7], Kenneth S. Johnson[8], Stephen C. Riser[3], and Osvaldo Ulloa[9]

1. *Institute of Biogeochemistry and Pollutant Dynamics, ETH Zurich, Zurich, Switzerland.*
2. *Woods Hole Oceanographic Institution, Woods Hole, MA, USA.*
3. *School of Oceanography, University of Washington, Seattle, WA, USA.*
4. *Department of Fisheries and Oceans, Institut Maurice-Lamontagne, Mont-Joli, Québec, Canada*
5. *Institute of Observational Research for Global Change and Japan Agency for Marine-Earth Science and Technology, Yokosuka, Japan*
6. *Leibniz-Institut für Meereswissenschaften at the University of Kiel, Kiel, Germany*
7. *NOAA Pacific Marine Environmental Laboratory, Seattle, WA, USA.*
8. *Monterey Bay Aquarium Research Institute, Monterey, CA, USA.*
9. *Departamento de Oceanografía & Centro de Investigación Oceanográfica, Universidad de Concepción, Concepción, Chile.*

Version 5-1, February 14, 2007
Prepared for distribution to the Argo Steering Committee

Summary

This white paper justifies and outlines a new international joint *Argo-Oxygen* program in order to determine, on a global-scale, seasonal to decadal time-scale variations in sub-surface dissolved oxygen concentrations. We propose to achieve this goal by adding dissolved oxygen sensors to the floats of the successful Argo array, thus extending its measurement capabilities. This *Argo-Oxygen* program is motivated by the fact that oceanic dissolved oxygen concentration is a key quantity for ocean ecology and biogeochemistry. It permits study and quantification of a diverse and crucial set of processes. These processes include the detection of the oceanic impact of global warming on ocean biogeochemistry and circulation, the addition of unprecedented constraints on the export of biologically formed organic matter, and improved estimates of the oceanic uptake of anthropogenic CO_2. The addition of oxygen to the currently measured suite of temperature and salinity on Argo will represent a revolutionary step in our ability to observe the ocean's evolution over time, integrating biogeochemical and physical observations.

This prospect is made possible by the success of the Argo program and the recent development of dissolved oxygen sensors that are both precise and stable over extended periods and can be easily integrated with the currently used Argo floats. Achieving the main goal of the *Argo-Oxygen* program does not require any appreciable changes in the deployment and operating strategies of the current Argo program and can therefore be implemented without significant negative impacts on the Argo core mission. Experience with the more than 70 Argo floats that have already been deployed with dissolved oxygen sensors suggests that the technology is ready for a first large-scale experiment, but that further evaluation and testing is needed before a global implementation is possible.

We therefore propose that the *Argo-Oxygen* program be implemented in two phases. In the pilot phase, one or two test regions will be seeded extensively with floats, many of which will contain two oxygen sensors. The region's oxygen distribution will then be repeatedly sampled using shipboard measurements over a period of two years in order to determine accurately the long-term changes in sensor accuracy and precision. Network optimization studies as well as first attempts at ingesting the data into diagnostic models will complete the pilot phase. The global implementation will build on the experiences gathered during this pilot phase and will take advantage of the network optimization studies aimed at determining the optimal number of oxygen sensors required to achieve the scientific goals.

The costs of the proposed *Argo-Oxygen* program must be fully borne by new funds that will have to be raised over and above the core funding of Argo. The cost will depend on the yet-to-be-determined size of the program (the number of floats with oxygen sensors) and the additional costs per Argo float with an oxygen sensor. The latter costs are determined by the cost of the oxygen sensor, as well as the costs that arise from the increased energy demand affecting the float life time, the costs associated with the likely required calibration of the oxygen sensor, and the costs of communication, data handling, data quality control, and data storage. Based on current technology and experience, the total lifetime cost of an Argo float with oxygen is estimated to be roughly 40% higher than that of a standard Argo float.

The proposed program will add substantial value to Argo by significantly broadening the scientific scope and expanding the number of Argo data users, as well as by creating new synergies between the physical and the biogeochemical ocean research communities. The new observations will also contribute to the activities of various international networks and partnerships for Earth Observing Systems, such as the Climate Observing System/Global Ocean Observing System GCOS/ GOOS.

Table of Contents

1 Introduction: The Argo-Oxygen program as a revolutionary step in ocean biogeochemistry

The oceans are warming. Between 1955 and 1998, the ocean's 0–3000 m heat content is estimated to have increased by a total of 145×10^{21} J, corresponding to a mean temperature increase of 0.037ºC (Levitus *et al.,* 2005). Projections of the future evolution of Earth's climate system suggest that this past warming is small relative to what can be expected by the end of this century. While the consequences of this heat uptake on steric sea-level rise are thought to be relatively well-known, the impacts of this heat uptake on ocean circulation, ocean biogeochemistry, and biology are not as well established. One important reason for this limited understanding is the chronic spatial and temporal undersampling of the ocean. Satellite missions have helped to alleviate this problem, but their sampling is restricted to near sea-surface or depth-integrated properties, such as sea-surface temperature or height. Ships of opportunity have also helped to extend the reach of oceanographic research ships to probe the ocean's interior, but only the advent of the Argo program at the turn of the century has made the ocean's interior accessible to observations at adequate temporal and spatial scales (e.g. Gould *et al.,* 2004). As Argo approaches the 3000 float plateau, the program is widely viewed as a great success, since it allows, for the first time, continuous monitoring of the temperature, salinity, and velocity of the upper ocean. Currently, there are nearly 2800 Argo floats operating in the ocean (Figure 1), bringing the array very close to its target size of 3000 floats. These floats measure temperature and salinity every 10 days, and the data are relayed and made publicly available within hours after collection through satellite communication and an advanced data management program.

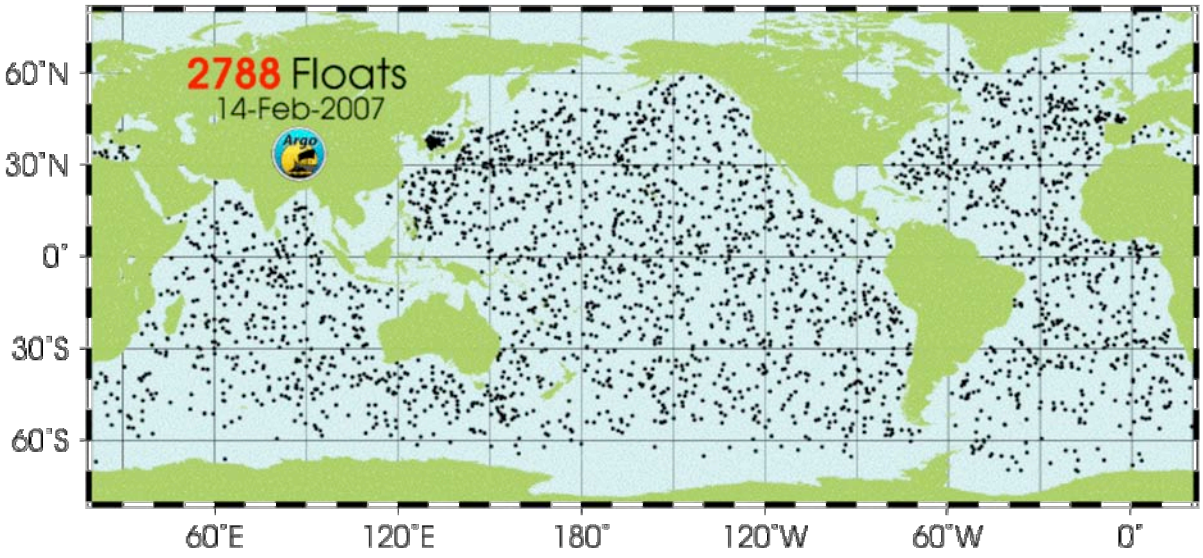

Figure 1: Status of the global Argo observing network as of 14 February 2007. Shown are the positions of the 2788 Argo floats that have reported data within the 30 day period before that date. From *http://www.argo.ucsd.edu*.

This dramatic increase in oceanographers' capability to observe the physical state of the ocean in near real time has not yet been paralleled by similar advances in observations of the large-scale biogeochemical and biological state of the ocean. At present, the primary mode of observing the ocean's interior evolution of biogeochemically and biologically relevant

properties is by sampling from research vessels. To date, the most ambitious international program to map out the distribution of biogeochemical tracers in the ocean was the global CO_2 survey undertaken jointly by the World Oceanographic Circulation Experiment (WOCE), the Joint Global Ocean Flux Study (JGOFS), and a few other national programs (Wallace, 2001). This survey, which took a decade to complete, resulted in the order of 100,000 biogeochemically relevant measurements, increasing the total number of observations for many parameters up to tenfold. However, this survey was largely a one-time snapshot, providing limited information about temporal evolution. Subsequently, a new international program was launched – the Repeat Hydrography Program – but despite very substantial international efforts, the average time between repeats of hydrographic sections is about a decade, with large parts of the ocean not being sampled at all (Fig. 2).

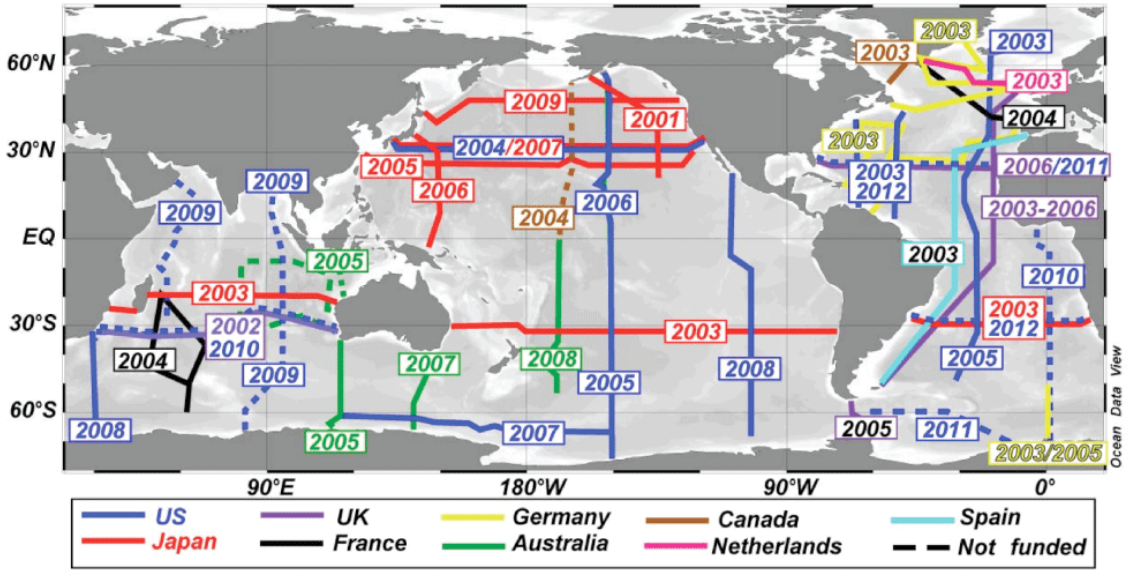

Figure 2: Current status of the global ocean repeat hydrography program (status early 2006). See *http://ioc.unesco.org/ioccp/Hydrography/Hydro_Map.htm* for planned cruises, and *http://cdiac.ornl.gov/oceans/RepeatSections/repeat_map.html* for executed cruises.

This repeat cycle and sparse spatial sampling may be adequate for determining the long-term increase of the oceanic carbon content in response to the increase of atmospheric CO_2 or for characterizing the uptake and subsequent redistribution of bomb radiocarbon (Bender *et al.*, 2002; IMBER/SOLAS, 2006), but a decade is substantially longer than the seasonal to sub-decadal time-scale that characterizes much of the thermocline variability in many biogeochemical parameters, as exemplified by the rapid changes in thermocline oxygen concentrations seen in the northeastern North Atlantic along 20ºW (Fig. 3). In addition, the relatively coarse spatial separation between sections is likely to be barely adequate to resolve sub- basin-scale variations in gyres and their water properties.

These undersampling problems could be easily overcome if biogeochemical or biological sensors could be added to profiling floats. If only 20% of the 3000 Argo floats were equipped with biogeochemical/biological sensors, more than 20,000 profiles with 1,500,000 or more measurements in the upper 2000 m could be made in a single year. In one year, the number of biogeochemical/biological profiles collected would reach the number of CTD stations

occupied during the ambitious WOCE one-time hydrographic survey. Furthermore, these profiles would be evenly distributed throughout the year, and could also be evenly distributed spatially. They would thus provide a three-dimensional synoptic and time-dependent picture of the global distribution of the measured biogeochemical/biological parameter(s). This array would hence overcome the limitations of the spatial and temporal aggregation of measurements typical for campaign-mode observations.

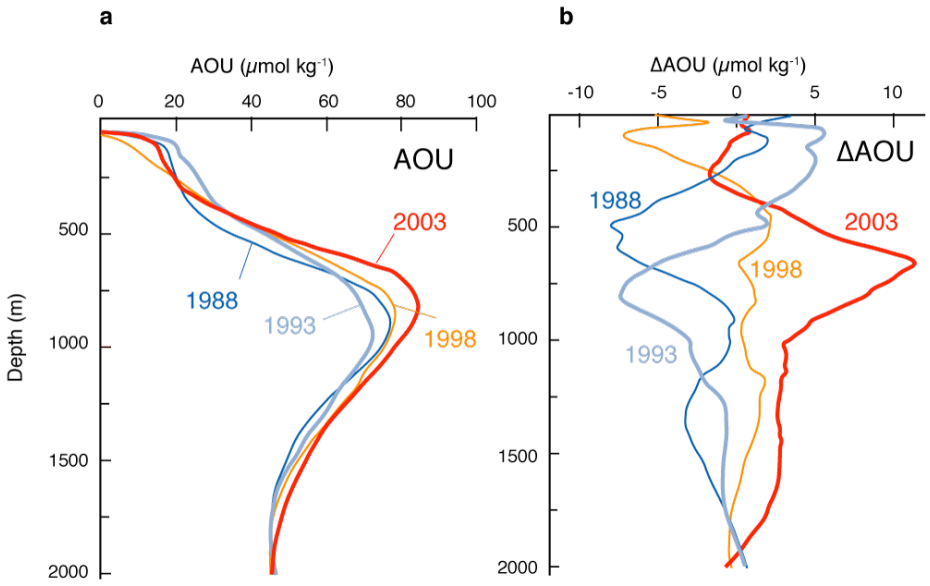

Figure 3: Time evolution of the Apparent Oxygen Utilization (AOU) in the North Atlantic from 1988 until 2003, averaged from 40ºN to 64ºN along 20ºW (AOU = $[O_2]^{sat} - [O_2]^{measured}$). (a) Mean profiles of AOU for the four occupations of the 20ºW line from 1988 through 2003. (b) Difference from the mean AOU profile of all 4 cruises. From *Johnson and Gruber* (in press).

However, until very recently, such biogeochemical/biological sensors suitable for use on Argo-type floats were not available. The rapid recent development in sensor technology (Johnson *et al.*, 2007) makes the expansion and augmentation of the Argo network for biogeochemistry/biology now possible. By far the most advanced sensors in terms of development and long-term experience with deployment on Argo floats are those for dissolved oxygen (O_2) (Fig. 4). Polarographic oxygen sensors have been deployed on Argo floats since at least as early as 2002. Published studies (Körtzinger *et al.*, 2004, 2005; Tengberg *et al.*, 2006) have also demonstrated the feasibility of a new instrument technology, the Optode, which takes advantage of dynamic luminescence of luminophores that fluoresce depending on O_2. For example, two prototype oxygen Optode instruments were deployed on autonomous floats in the Labrador Sea in September 2003, and data collected over the following year showed very promising results that demonstrated high accuracy and stability (Körtzinger *et al.*, 2004; Tengberg *et al.*, 2006). Several Argo floats have been deployed equipped with both types of O_2 sensors, bringing the total number of floats equipped with one or more O_2 sensors to 75 as of November 2006.

This white paper aims to develop and present the scientific justification as well as the practicality of adding O_2 sensors to the Argo array in order to determine the seasonal to decadal time-scale variations of the ocean's oxygen content. The *Argo-Oxygen* program will constitute an order of magnitude or more increase in our ability to observe the

biogeochemical state of the ocean, with repercussions and benefits for many other aspects of oceanography.

Figure 4: Photo of the top cap of a profiling float with the two most advanced oceanographic oxygen sensors installed side by side: The SeaBird Electronics Inc. SBE-43 electrochemical sensor is on the left, with the Aanderaa Optode sensor on the right. Field results from such dual-sensor floats are already available. (Photo from S. Riser)

Why is a full-fledged observatory of oxygen in the ocean needed? As Joos *et al.* (2003) pointed out, the (mostly) decreasing trends in the concentrations of dissolved oxygen in the ocean over the last few decades (e.g. Emerson *et al.*, 2004) have important implications for our understanding of anthropogenic climate change. As sub-surface oxygen concentrations in the ocean everywhere reflect a balance between supply through circulation and ventilation and consumption by respiratory processes, the absolute amount of oxygen in a given location is therefore very sensitive to changes in either process, more sensitive, perhaps, than other physical and chemical parameters. Oceanic oxygen has therefore been proposed as a bellwether indicator of climate change, analogous to the canary in the coal mine (Joos *et al.,* 2003; Körtzinger *et al.,* 2006)

But an enhanced oxygen observatory in the ocean can do even more for us: It will improve the atmospheric O_2/N_2 constraint on the ocean-land-partitioning of anthropogenic CO_2, a much sought-after quantity (Keeling *et al.*, 2002). Annual cycles in oxygen concentration that are observed below the euphotic zone will also allow determination of the seasonal to interannual net remineralization rates as a proxy for export production (Najjar and Keeling, 1997). This quantity is currently not well constrained. It should help interpretation of variations in water mass ventilation rates and will provide crucial data (initial conditions, evaluation) for ocean biogeochemistry models. It will aid interpretation of sparse data from repeat hydrographic surveys that are needed, for example, to constrain the oceanic inventory of anthropogenic CO_2. This list of benefits, while not exhaustive, is certainly sufficient to warrant a major international attempt to quantify seasonal to decadal-time changes in sub-

surface oceanic oxygen storage and transport, a task that can be efficiently achieved by augmenting many floats in the Argo array with oxygen sensors.

Oceanic measurements of dissolved oxygen have a long history, and oxygen is the third-most oft-measured water property (behind temperature and salinity). Realizing the tremendous utility of oxygen measurements in the ocean, an informal "Friends of Oxygen" initiative was formed in 2005 to bring oceanic oxygen measurement into the 21st century by advocating the widespread deployment of oxygen sensors on profiling floats. From this group, with encouragement from IOCCP and the Joint IMBER-SOLAS Carbon Research Group, a writing team emerged with the goal to put together this White Paper for the promotion of the addition of oxygen sensors to the international Argo float program. This white paper is only a first step, Clearly, substantial additional work will be required, including more careful assessments of the feasibility of high-quality long-term measurements of oxygen from floats as well as more detailed estimates of the associated costs. However, we are convinced that the *Argo-Oxygen* program will significantly increase the scientific merit of Argo and also attract a whole new community of data users. By joining forces under the Argo sail, oceanographers from various parts of the community could foster a renaissance of oxygen as a classical oceanographic parameter, helping us identify and understand global climate change.

2 Scientific Objective

The key scientific objective of the *Argo-Oxygen* program is

To determine seasonal to decadal-time variability in sub-surface ocean oxygen storage and transport on a global scale.

As the temporal and spatial scales of oxygen variability are similar to those of temperature, and the Argo array is designed to achieve these objectives for temperature, they can be achieved for oxygen by extending the presently operating global Argo program to include oxygen sensors on their floats, without requiring any changes in the operating cycle of the floats. However, achieving these objectives requires accurate and precise long-term measurements of the dissolved oxygen concentration as outlined in more detail below.

3 Scientific rationale

3.1 Detect changes in ocean biogeochemistry and climate

Model simulations indicate that the ocean's oxygen content will respond very sensitively to global ocean warming, with the magnitude of the outgassing flux exceeding that expected on the basis of the solubility decrease (Bopp *et al*, 2002; Plattner *et al*., 2002, etc). This prediction is a result of biologically/physically induced changes in the oxygen outgassing flux, which tend to act in concert with those induced by heating/cooling (Gruber *et al.,* 2001). In fact, the total outgassing flux (and corresponding decrease in the ocean's oxygen content) is predicted to be about 3 to 4 times larger than that expected based on the solubility decrease alone (Manning and Keeling, 2006) (Fig. 5). This result contrasts with oceanic CO_2, where

biologically/physically induced changes tend to act in the opposite direction on the air-sea exchange of CO_2 in comparison to the changes induced by heating/cooling. As a result, the changes in the air-sea CO_2 flux expected from a given heat input into the ocean are difficult to predict and tend to be very model dependent.

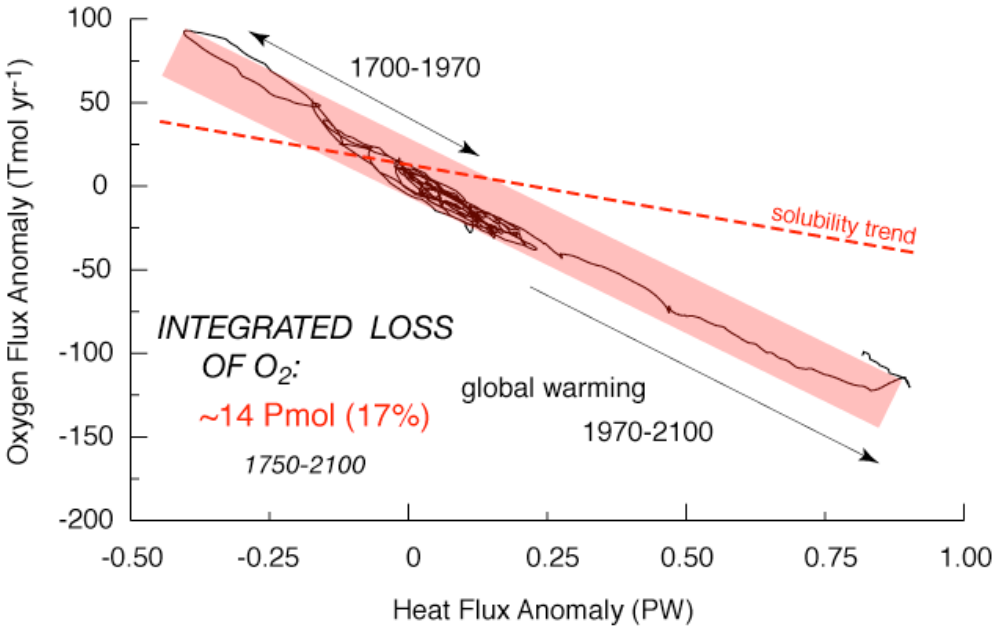

Figure 5: Modeled evolution of the anomalous air-sea flux of oxygen from 1750 until 2100 in relationship to the anomalous air-sea flux of heat (abscissa). Over the period from both 1700 until 1970 and 1970 until 2100 the anomalous air-sea flux of oxygen is highly linearly correlated with that of heat. The amount of outgassing of O_2 for a given heat uptake by the ocean is simulated to be about 3 to 4 times larger than the reduction in oxygen solubility would predict (red dashed line). In this particular model simulation, 14 Pmol of O_2 is lost from the ocean between 1750 and 2100, corresponding to a 17% reduction in the oceanic oxygen content. These large changes as well as the high sensitivity of oceanic oxygen to climate forcing make oxygen an ideal candidate for detecting the impact of global climate change on ocean biogeochemistry. Based on results of Plattner *et al.* (2002).

The expected oxygen loss from the ocean in response to global warming can be quite substantial. For example, using a relatively simple ocean biogeochemical model coupled to a climate model, Plattner *et al*. (2002) predict by 2100 a total oxygen loss of about 14 Pmol of O_2, representing a 17% reduction of the ocean's oxygen content. This substantial reduction in the mean oxygen content is accompanied with a substantial increase in the extent of the oxygen minimum zones. Some model simulations (Matear and Hirst, 2003) suggest a doubling of the regions with suboxia ($O_2 < 10$ μmol kg^{-1}), i.e. a doubling of the marine "dead-zones" with severe implications for all higher life-forms and for long-term nutrient inventories and cycles (e.g., loss of fixed nitrogen via enhanced denitrification, or possible gain of iron and phosphorus through the sediment-water interface).

Given the large oxygen changes expected in response to global warming and the high precision and accuracy with which oxygen can be measured, the signal to noise ratio is excellent, making oxygen a prime candidate to act as a sensitive metric for detecting climate change in the ocean (e.g. Deutsch *et al*. 2005).

Presently available observations of the long-term evolution of the ocean's oxygen content largely show decreases in the oxygen content (Fig. 6, Johnson and Gruber, in press; compare

Fig. 3; Deutsch *et al.*, 2005, 2006; Emerson *et al.*, 2004; Shaffer *et al.*, 2000; Matear *et al.*, 2000; Bindoff and McDougall, 2000; Andreev and Watanabe, 2002; Watanabe *et al.*, 2001; Ono *et al.*, 2001; Garcia *et al.*, 1998; Keller *et al.*, 2002), consistent with the expected trend based on the ocean's warming. However, there are also regions where oxygen has increased recently such as the southern Indian Ocean (Mcdonagh *et al.*, 2005), possibly reflecting natural variability in the oceanic system. The lengths of the records and the small number of regions with repeat sampling make it impossible to extrapolate these observations to larger regions or even to the globe in order to assess the global-scale oxygen balance of the ocean.

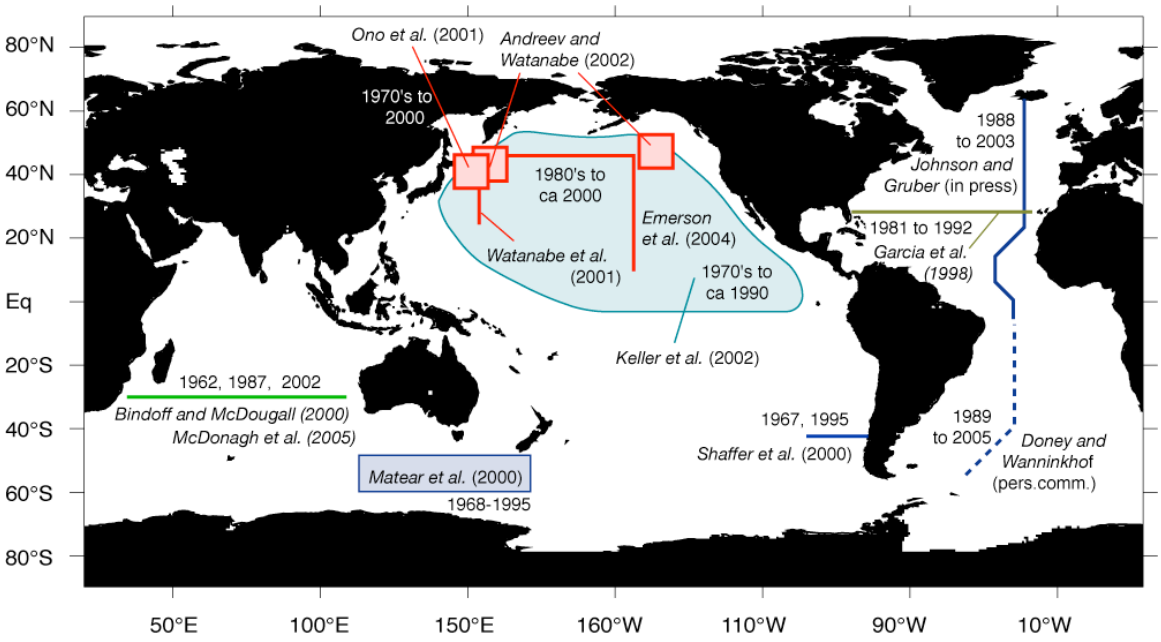

Figure 6: Summary of studies that have reported long-term changes in the ocean's oxygen content. The majority of these studies show long-term decreases in the oceanic oxygen concentration, particularly in the mid-thermocline (see e.g. Fig. 3), consistent with the trend expected from global warming. However, the records are too short and too sparse to draw any firm conclusions.

The addition of oxygen sensors to the Argo array would in a few years alleviate the overwhelming undersampling problem (Fig. 6) for oxygen. However, the requirement to detect long-term changes in oceanic oxygen also places serious demands on the accuracy and long-term stability of the oxygen sensors. The trends that have been reported so far are of the order of a few μmol kg^{-1} yr^{-1}, i.e. generally less than 1% yr^{-1}. Thus the oxygen sensors need to exceed this long-term stability and accuracy in order to provide, by themselves, the necessary quantitative constraint on the long-term evolution of the ocean's oxygen content. Combining the oxygen fields estimated from the *Argo-Oxygen* program with the more accurate O_2 measurements from the repeat hydrography program may alleviate this constraint somewhat

3.2 Improve atmospheric O_2/N_2 constraint on ocean/land partitioning of anthropogenic CO_2

Simultaneous measurements of O_2/N_2 and CO_2 in the atmosphere are one of the most powerful tools to determine the fate of the fossil fuel emitted into the atmosphere (Keeling and Shertz, 1992; Keeling *et al.*, 1996; Manning and Keeling, 2006). As a result, this method

has been adopted by the Intergovernmental Panel on Climate Change (IPCC) as one of the key methods to separate that part of the fossil-fuel CO_2 emissions that is being taken up by the ocean from that part that is taken up by the terrestrial biosphere. This method hinges critically on the assumption that the oceanic uptake of anthropogenic CO_2 occurs in the absence of a net global air-sea exchange of oxygen, while the anthropogenic CO_2 uptake by the terrestrial biosphere is accompanied by a stoichiometric release of oxygen. This assumption is well justified for the oceanic uptake of anthropogenic CO_2. However, the recent warming of the ocean (Levitus *et al.*, 2000, 2005) has led to an outgassing of oceanic oxygen, which needs to be accounted for in the method in order to correctly attribute the anthropogenic CO_2 sinks to the land and ocean (Fig. 7).

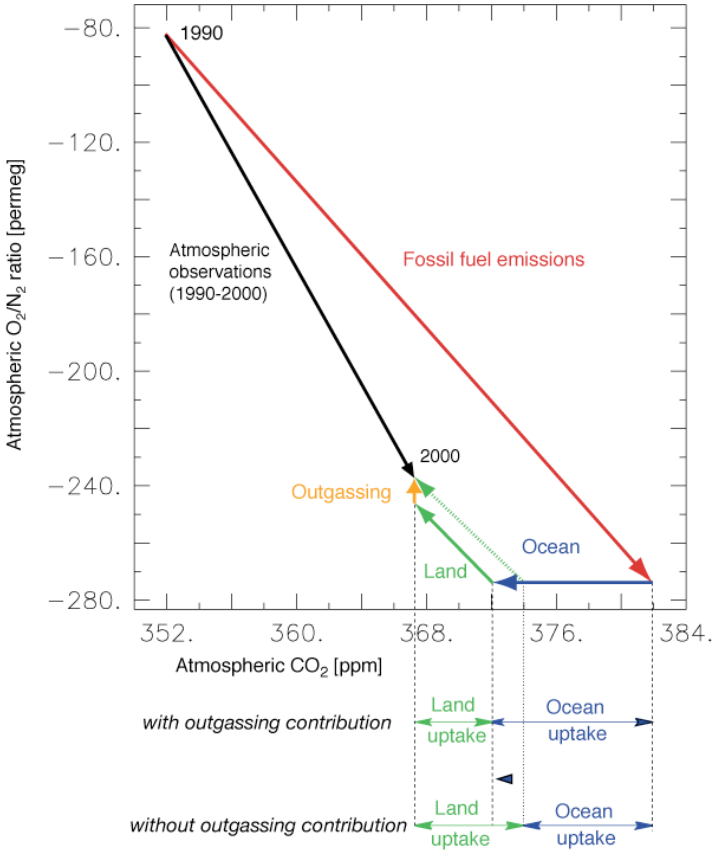

Figure 7: Impact of the oceanic outgassing of oxygen on the atmospheric O_2/N_2 method for determining the sinks for anthropogenic CO_2. The diagram shows the observed temporal evolution of the atmospheric O_2/N_2 ratio versus that of atmospheric CO_2 (black arrow) as well as the different contribution to the global budget for CO_2 and O_2, i.e. fossil fuel emissions (red arrow), oceanic uptake (blue arrow), land uptake (green arrow), and oceanic outgassing of oxygen (orange arrow). Any uncertainty in the outgassing of oceanic oxygen leads to a nearly corresponding uncertainty in the partitioning of the anthropogenic CO_2 fluxes between the ocean and the land biosphere.

This oceanic outgassing is currently estimated on the basis of the observed increase in the ocean's heat storage assuming a fixed scaling between the anomalous air-sea flux of heat and that of oxygen, i.e. the slope of the relationship shown in Fig. 5 (Keeling and Garcia, 2002; Manning and Keeling, 2006; Plattner *et al.* 2002; LeQuéré *et al.* 2003, Bopp *et al.* 2002). The various studies use considerably different estimates of this scaling, leading to substantial differences in the estimated oxygen outgassing with corresponding differences in the magnitude of the proposed correction. The magnitude of this correction is one of the largest

sources of uncertainty in the partitioning, as any uncertainty in the estimated oxygen outgassing leads to a nearly corresponding uncertainty in the estimated uptake by the ocean and/or land biosphere. Direct determination of changes in the oceanic oxygen reservoir therefore would substantially reduce a major source of uncertainty for this method. Despite the challenges posed by the oceanic oxygen outgassing, the atmospheric O_2/N_2 method will remain an important method in the future, since this is the only method that can alert us rapidly if major changes occur in the either the oceanic or land biosphere uptake of anthropogenic CO_2. All other methods to determine this uptake rely on in-situ oceanic CO_2 measurements, which can take many years to accumulate and synthesize before any trends in the uptake can be seen.

Thus, direct measurements of changes in the oceanic oxygen content would provide very valuable benefits for the understanding of the global carbon cycle. The determination of the spatial distribution of the long-term changes in oceanic oxygen will also permit researchers to determine where and when the anomalous oxygen fluxes have occurred (see 3.7), providing additional benefits to the interpretation of the atmospheric oxygen records. As was the case with the use of oceanic oxygen to detect the impact of climate change on the ocean, this scientific objective requires high accuracy measurements over extended periods of time.

3.3 Determine seasonal to interannual changes in oxygen in sub-mixed layer waters as a proxy for net community production and export production

Biological mechanisms that transfer organic carbon from the surface ocean have an important influence on atmospheric CO_2 and thus global climate. This flux—the ocean's carbon pump—has been characterized in only a few ocean areas because an accurate estimate of the net annual biological oxygen production in the euphotic zone or the consumption rate below the euphotic zone requires a time series of measurements and there are only a handful of ocean areas where this has been done (e.g., Emerson *et al.*, 1997).

In mid- to high latitudes, a seasonal maximum in subsurface oxygen saturation can develop in the seasonal thermocline because of the interplay of enhanced photosynthetic biological production, shallower mixed layer depths, and warming temperatures over the spring and summer (e.g., Najjar and Keeling, 1997). These seasonal changes have been used to estimate the annual rate of net biological oxygen production in regions of the ocean where time-series of measurements have been made. The annual oxygen production is stoichiometrically related to the annual flux of carbon out of the euphotic zone. While there are complications caused by estimating fluxes of gas at the air-water interface by both diffusive and bubble mechanisms and into the top of the thermocline by intermittent mixing processes, this method has resulted in among the most accurate measures of the biological pump (Spitzer and Jenkins 1989, Emerson *et al.* 1997).

Immediately below the ocean's euphotic zone, oxygen is consumed by net heterotrophic respiration. Since most of the organic matter that exits the euphotic zone is oxidized in the top several hundred meters, the integrated decrease of oxygen in this region, accompanied by an estimate of the time since it was at the surface, is also a measure of the strength of the biological pump (Jenkins and Doney 2003). Analyses of the historical oxygen database in the World Ocean Atlas by Najjar and Keeling (1997) demonstrate an annual cycle in oxygen concentration at depths below the euphotic zone and at latitudes poleward of 30°. This cycle is mostly driven by seasonal changes in carbon export, respiration and ventilation. An array

of oxygen sensors on floats would allow the amplitude of this cycle to be constrained geographically and temporally. This seasonal signal would provide an additional constraint on oxygen consumption rates and carbon export.

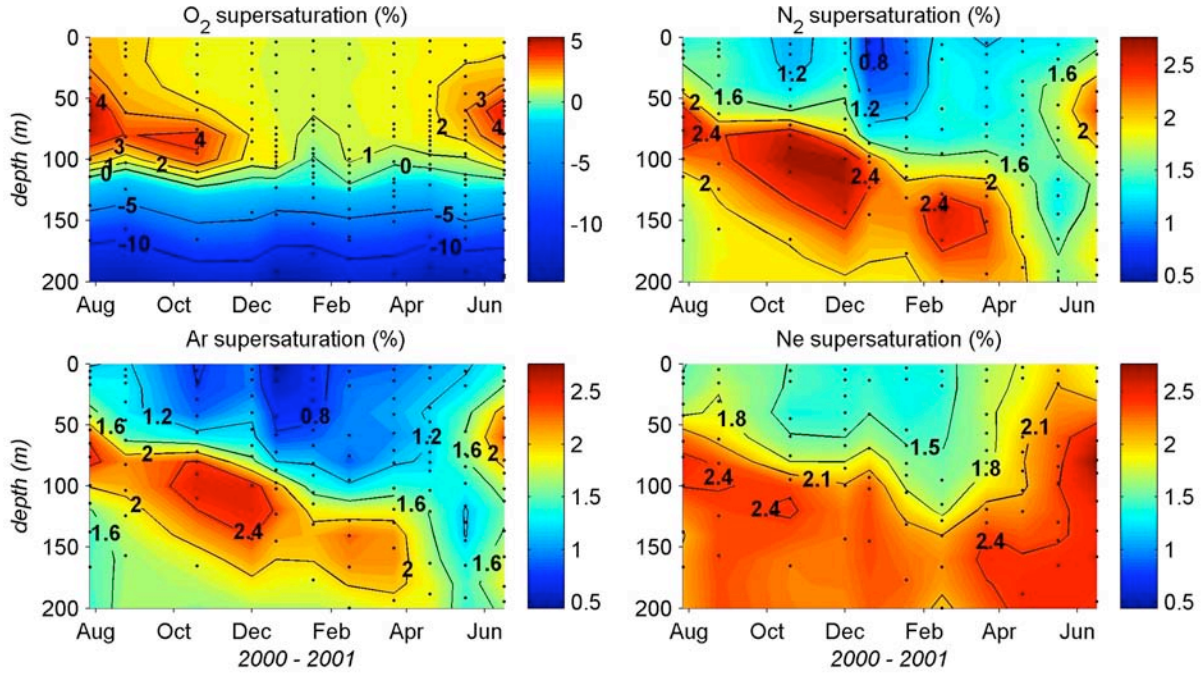

Figure 8: Measurements of gas saturations from the Hawaiian Ocean Time Series (HOT) site ALOHA near Hawaii from August 2000 – June 2001. Shown are shipboard-based measurements of the saturation state of (a) oxygen, (b) nitrogen, (c) argon, and (d) neon (data from S. R. Emerson).

If Argo Floats are equipped with oxygen sensors that are accurate enough to determine the O_2 concentration to better than 1%, and with a response time fast enough to resolve the rapid vertical variations in oxygen, it will be possible to dramatically increase the number of ocean areas with sufficient oxygen measurements to determine the net annual biological carbon export. These observations are essential to calibrate global estimates of carbon export inferred from satellite color measurements (e.g., Laws *et al*., 2000) and global circulation models (Jin *et al*, 2007).

3.4 Aid interpretation of variations in ocean circulation/mixing

Analyses of the distribution of oxygen have been used for decades by physical oceanographers to infer pathways and rates of ocean circulation and mixing. Among the first to take advantage of the unique properties of oxygen was Wüst (1936), who used it together with his temperature and salinity measurements from the German *Meteor* expedition in 1925–1927 to describe the unique vertical structure of water masses in the Atlantic and to infer their sources and flow pattern. As elucidated above, the key usefulness of oxygen for ocean circulation studies is that it contains information about the age of the water parcel, since in the ocean's interior there are no sources of oxygen, only sinks.

In the ocean interior, away from major current systems, eddies dominate the flow field. With long-term mean currents several times smaller in magnitude than eddy motions, it is usually difficult to make reliable maps of mean ocean currents on isopycnal surfaces from direct

current measurements. In this context, maps of oxygen concentration on isopycnal surfaces provide valuable information on flow direction. They could even allow estimates of mean flow velocities subject to better constraints on the spatially dependent oxygen utilization rates. In the process of water mass formation in the subtropical convergence zones, isopycnals outcrop at mid-latitudes and get oxygenated (though not exactly at 100% saturation) during major winter mixing events. As these newly oxygenated waters subduct and leave the region of surface winter mixing, they become isolated from the atmosphere and start losing oxygen due to respiration and organic matter mineralization. A rough indicator of flow direction, from high oxygen regions to low oxygen regions, can then be obtained by examining oxygen gradients on isopycnal surfaces. Oxygen concentrations tend to respond very quickly and sensitively to changes in ocean circulation (e.g., Shaffer et al., 2000). In fact, most of the observed O_2 changes in the ocean can be traced back to variations in ocean circulation rather than changes in ventilation or oxygen utilization rates (see e.g. Deutsch *et al*., 2005).

Oxygen can also be very useful in the study of deep convection in the North Atlantic and around Antarctica, as demonstrated from a small pilot study in the Labrador Sea (Körtzinger *et al*. 2004, 2005). Very weak vertical gradients of temperature and salinity in regions of active convection yield ambiguities about the depth of vertical mixing. Such ambiguities may be removed with oxygen data as an additional measured parameter, since ventilating waters should have uniform oxygen values (Körtzinger *et al*. 2004). Depending on dominant winter storm tracks that change from year to year and lead to changes in the North Atlantic Oscillation (NAO) index, the most active sites of winter convection in the North Atlantic can unexpectedly shift from the Labrador Sea to the Irminger Sea and/or the Greenland/Icelandic/Norwegian (GIN) Seas. Given the very low predictability of the NAO index on time scales longer than about a month (Mosedale *et al*., 2006), any study of winter deep convection in the North Atlantic would require the simultaneous deployment of oxygen floats in the Labrador, Irminger and GIN Seas.

Finally, we note that while oxygen has been used in quantitative water mass analysis for decades (Tomczak 1999), physical oceanographers are increasingly making use of nutrients and other chemical parameters in optimal multiparameter analysis to provide estimates of water mass age (Karstensen and Tomczak 1998) or to help diagnose temporal changes in water mass properties (Henry-Edwards and Tomczak 2006).

3.5 Provide constraints for ocean biogeochemistry models

Ocean biogeochemistry models have notorious problems matching the observed spatial distribution of oxygen in the ocean interior, reflecting an inability of the models to properly capture the interplay between ventilation rates and biological uptake via organic matter respiration (e.g., Najjar *et al*., submitted). Simulated oxygen distributions in the mid- and lower-thermocline in the OCMIP-2 intercomparison study varied by more than 100 μmol kg^{-1} (±50% of the observed value) in the global mean at a particular depth across the suite of models. There has been less exploration of model skill on replicating the seasonal cycle of oxygen (e.g., Jin *et al*., in press) and interannual variability, but experience with the mean state indicates the likely presence of similar difficulties. These large model errors currently limit the usefulness of the present day simulations for applications to interannual climate variability and global change questions.

Turning the problem around, however, these large model-data discrepancies suggest that oxygen could provide an invaluable measure for assessing model performance and conducting ocean inversion studies to improve model parameterization. Some experiments have even shown that simulated oxygen distributions may be more sensitive, in unexpected ways, to changes in model dynamics and model parameters than nutrients such as phosphate (e.g., Anderson and Sarmiento, 1995). As already mentioned, an *Argo-Oxygen* program would provide invaluable data on the seasonal dynamics in the euphotic zone and upper aphotic zone as well as on the vertical gradients of oxygen through the thermocline, where most of the organic particle remineralization occurs. Many ocean biogeochemical models now include explicit treatment of denitrification in water column oxygen minimum zones, and thus improved information on the mean distribution and variability of the boundaries of these oxygen minimum zones could be combined with model circulation fields to better quantify a key aspect of the ocean nitrogen cycle. An observing system like *Argo-Oxygen* may provide the only feasible approach for initializing and evaluating forward model simulations of interannual ocean biogeochemical variability in a comprehensive fashion. On a somewhat longer time horizon, we can anticipate the development of biogeochemical modules for ocean data assimilation models, which would naturally merge improved model dynamics and time-evolving ocean observations.

3.6 Aid in interpretation of sparse data from repeat hydrographic surveys

Occupations of repeat hydrographic sections occur only once every decade at best. Thus while repeat surveys provide temporal snapshots for a rich suite of physical and chemical tracer data (O_2, nutrients, inorganic carbon system, transient tracers), there is often little information available to aid in deciphering how much of these observed differences is due to variability on shorter, subseasonal to interannual time-scales (e.g., Doney *et al.*, 1998; Johnson and Gruber, in press) versus the desired longer-term secular trends associated with climate change and the uptake of anthropogenic CO_2. Quasi-continuous oxygen measurements from Argo, although less accurate and precise than those obtained by shipboard measurement, will fill in these gaps and permit an improved understanding of these changes in a nearly continuous time evolving manner. In return, the oxygen data from the repeat hydrographic survey will help to validate and perhaps even calibrate the float oxygen data.

Oxygen data from floats can also be used to better constrain changes in inorganic carbon properties determined from the repeat hydrographic program. To first order the subsurface fields of oxygen and dissolved inorganic carbon (*DIC*) co-vary because respiration of organic matter releases inorganic carbon while removing oxygen. This fact has been exploited using multi-parameter linear regression methods to extrapolate in space the relatively sparsely sampled inorganic carbon measurements using more densely sampled parameters such as oxygen (e.g. Wallace, 1995; Holfort *et al.*, 1998). It is also fundamental to several empirical approaches for removing the biological signal in the inorganic carbon field in order to estimate the anthropogenic carbon burden in the ocean and its evolution over time (e.g. Gruber *et al.*, 1996). The repeat hydrography program and an *Argo-Oxygen* network would thus complement each other whereby the regional information on the relationship between O_2 and *DIC* derived from sparse decadal scale ship-based survey could be applied to the more densely sampled Argo data to provide a more detailed perspective on the time-space evolution of *DIC* and anthropogenic carbon.

3.7 Determine transport and regional air-sea fluxes of oxygen

The transport and air-sea flux of oxygen are quantities of considerable interest as they provide strong constraints on biological productivity (Najjar and Keeling, 2000) and the large-scale oceanic transport of heat and CO_2 (Keeling and Peng, 1995; Stephens *et al.,* 1998; Gruber *et al.,* 2001; Battle *et al.,* 2006). Of particular relevance is the observation that atmospheric O_2, once corrected for the influence of the exchange of O_2 with the terrestrial biosphere using a tracer called atmospheric potential oxygen ($APO = O_2 + CO_2$ as in Stephens *et al.,* 1998) shows a substantial interhemispheric gradient with concentrations decreasing toward the north. This gradient requires an excess of oceanic oxygen sources over sinks in the southern hemisphere and vice versa in the northern, implying a transport of oxygen within the ocean from the northern hemisphere to the southern. The magnitude of this interhemispheric transport of oxygen in relationship to the oxygen sources and sinks could be somewhat modified by an interhemispheric transport of organic carbon, because the latter also causes sources and sinks of oxygen. However, the magnitude of the oxygen sources and sinks implied by the interhemispheric transport of organic carbon is generally considered small. Stephens *et al.* (1998) used APO to evaluate three global ocean carbon cycle models with regard to their simulations of O_2 fluxes across the air-sea interface. When they combined these fluxes with an atmospheric transport model, they found that all models significantly underestimated the interhemispheric gradient in APO. They interpreted this shortcoming as the result of an underestimation of the southward transport in the oceans.

Gruber *et al.* (2001) and more recently Battle *et al.* (2006) demonstrated, however, that this constraint might be weaker than originally thought, as substantial uncertainty exists with regard to atmospheric transport as well. Nevertheless, estimates of air-sea fluxes and oceanic transport of oxygen contain much information about ocean circulation and oceanic heat transport, which can be exploited as constraints for ocean circulation models as well as help to improve our understanding of high-latitude ventilation processes.

Air-sea fluxes of oxygen cannot be determined directly from the interior ocean oxygen measurements. However, they can be estimated from either simple budget calculations over a control volume or through the use of inverse techniques (Gruber *et al.*, 2001; Ganachaud and Wunsch, 2002). While the currently existing techniques are steady-state inversion methods, the availability of a 3-dimensional time-evolving picture of the oceanic oxygen content will permit researchers to develop temporally resolved methods. These methods will allow interannually varying transport and flux estimates at seasonal resolution. Such information, when coupled with atmospheric O_2 measurements, will provide also constraints for the exchange of oxygen (and carbon) with the terrestrial biosphere.

Another benefit of an improved characterization of the air-sea fluxes of oxygen is the opportunity to estimate the gas exchange coefficient and its dependence on environmental factors (Keeling *et al.,* 1998)

3.8 Prediction and assessment of anoxic or hypoxic events

Hypoxic or anoxic events in coastal waters represent a substantial threat to many coastal habitats, causing substantial environmental and economic damages (e.g. Service, 2004). Although coastal eutrophication is an important driver for such events, the initial oxygen

concentration of the deep-ocean waters advecting into the near-shore environments is an important determinant as well (e.g. Kasai et al., 2007). For example, an anomalous intrusion of Subarctic water into the California Current System led to unprecedented development of severe inner-shelf hypoxia along the Oregon Coast and resultant mass mortality of fish and invertebrates in summer 2002 (Grantham *et al.,* 2004). Gilbert *et al.* (2005) present evidence of a long-term decline of oxygen in the St. Lawrence Estuary (Canada) from intrusions of oxygen-poor oceanic water. Therefore, detailed measurements of the oxygen concentrations in the open ocean source waters will permit much better prediction and assessment of such hypoxic or anoxic events. Such hypoxic events may become more frequent in the future, as global warming increased stratification of the open ocean will tend to decrease the oxygen concentration of the waters that usually advect toward the shore. This process may underlie already part of the trend toward more intense, longer, and more frequent coastal hypoxic events that has been observed in the last few decades (Rabalais and Turner, 2001).

4 Showcase examples

To illustrate the technical capabilities and scientific opportunities for an *Argo-Oxygen* program, we discuss briefly two example field studies using in-situ oxygen sensors on autonomous ocean platforms, the first (Section 4.1) focused on the response of subsurface oxygen to gas exchange and deep-convective mixing in the Labrador Sea and the second (Section 4.2) on efforts to constrain the net biological production near Hawaii.

4.1 Deep ventilation of the Labrador Sea

A pilot study was initiated in 2003 to demonstrate the feasibility and scientific potential of float-based oxygen observations. This work was funded by the Collaborative Research Centre "Dynamics of Thermohaline Circulation Variability (Program: "Argo eq. IFM2") located at the IFM-GEOMAR in Kiel, Germany. Two APEX floats (Webb Research Corp., E. Falmouth/MA, USA), each equipped with an Aanderaa oxygen Optode and a Seabird CTD, were deployed side-by-side in Sept. 2003 in the central Labrador Sea, a region of deep convection subject to strong interannual and interdecadal variability (Körtzinger *et al.*, 2004).

One of the two floats quickly developed a problem with the pressure sensor and failed. The other float measured a total of 84 weekly vertical profiles of T, S, and O_2 in the upper 2000 m. It remained in the region of deep convection in the central Labrador Sea Gyre during the fall, winter, and spring (Fig. 9a), i.e., over a full deep convection event. O_2 profiles from this period (Fig. 9b) as well as T and S data (not shown) revealed the transition from a late-summer stratified water column (with a mixed-layer depth of <50 m) into a convectively overturning, deeply mixed late-winter situation (mixed-layer depth of 1400 m). This change was associated with an inventory increase in the upper 1400 m of 17 mol of O_2 m^{-2} (Fig. 9c), which corresponds to monthly air-to-sea fluxes of up to 7 mol of O_2 m^{-2}. Such fluxes strongly exceed those previously reported for the subpolar North Atlantic (Garcia and Keeling, 2001).

The oxygen intake was mostly driven by the progressive, almost exponential, deepening of the mixed layer (Fig. 9c), which exposed large volumes of undersaturated water to the atmosphere. This "deep breath" of a high-latitude deep convection region was observed in real time using satellite telemetry. The inhalation of oxygen stopped in early April (profile 30), when deep convection ceased. Afterward, the homogeneously mixed volume was rapidly capped by a shallow low-salinity surface layer and thus sealed from the atmosphere.

Subsequently, lateral intrusions into the newly formed water introduced spike-like signatures that likely represent characteristics of water from outside the convection region. The rapid decrease of the O_2 inventory after convection is striking. Outgassing can be ruled out as a major cause. Rather, it appears that the newly added oxygen is rapidly injected into the ocean interior through lateral export of the convectively mixed water and replacement with less oxygenated surrounding waters.

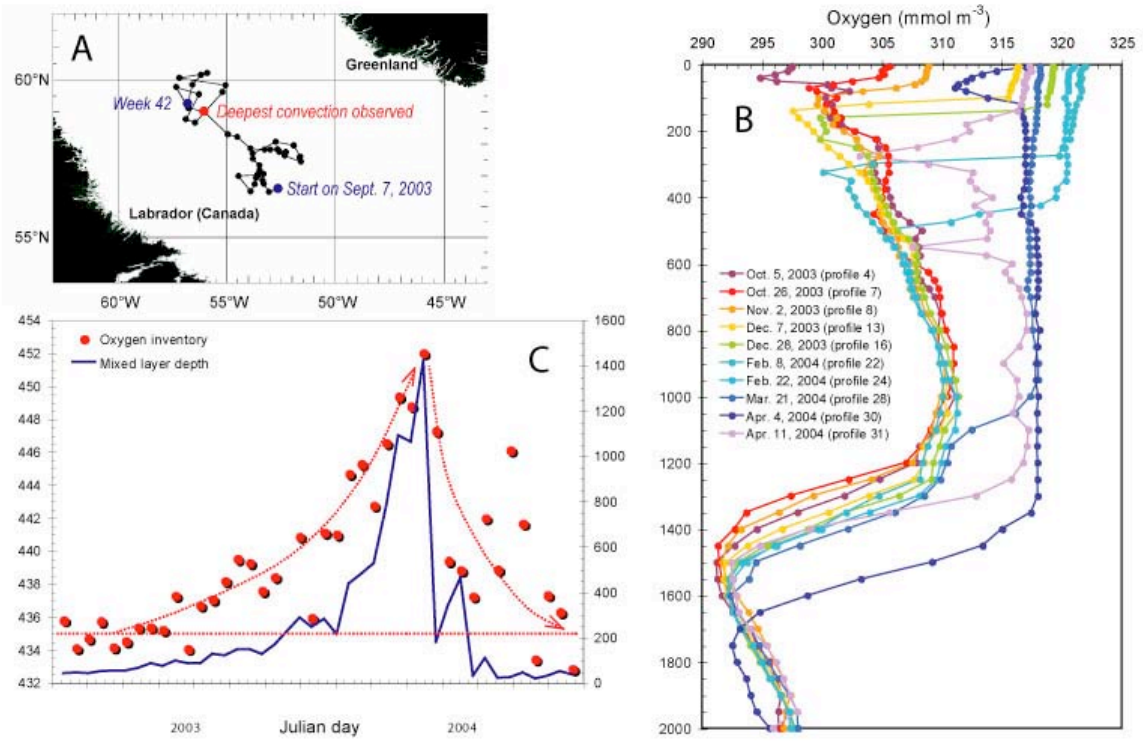

Figure 9: (a) Float track in the central Labrador Sea Gyre, showing positions of weekly surfacing between deployment on 7 September 2003 and profile 42 on 26 June 2004. (b) Selected vertical oxygen profiles. (c) Temporal development of the oxygen inventory (in the upper 1400 m) and mixed-layer depth, based on 42 weeks of measurements. Dotted red lines represent the build-up and decay of the oxygen inventory in the convection region relative to an assumed background concentration of the surrounding waters. From Körtzinger *et al.* (2004)

In a follow-up study, four APEX oxygen floats (with RAFOS tracking) were deployed in the Labrador and Irminger Seas in September 2004. All floats performed very well and delivered between 87 and 118 profiles (one float was still active in Dec. 2006). One float remained in the region of deep convection in the Labrador Sea for two consecutive convection season (2004/2005 and 2005/2006) and produced another interesting time-series of convection-driven variations in the oxygen inventory of the upper Labrador Sea (Fig. 10).

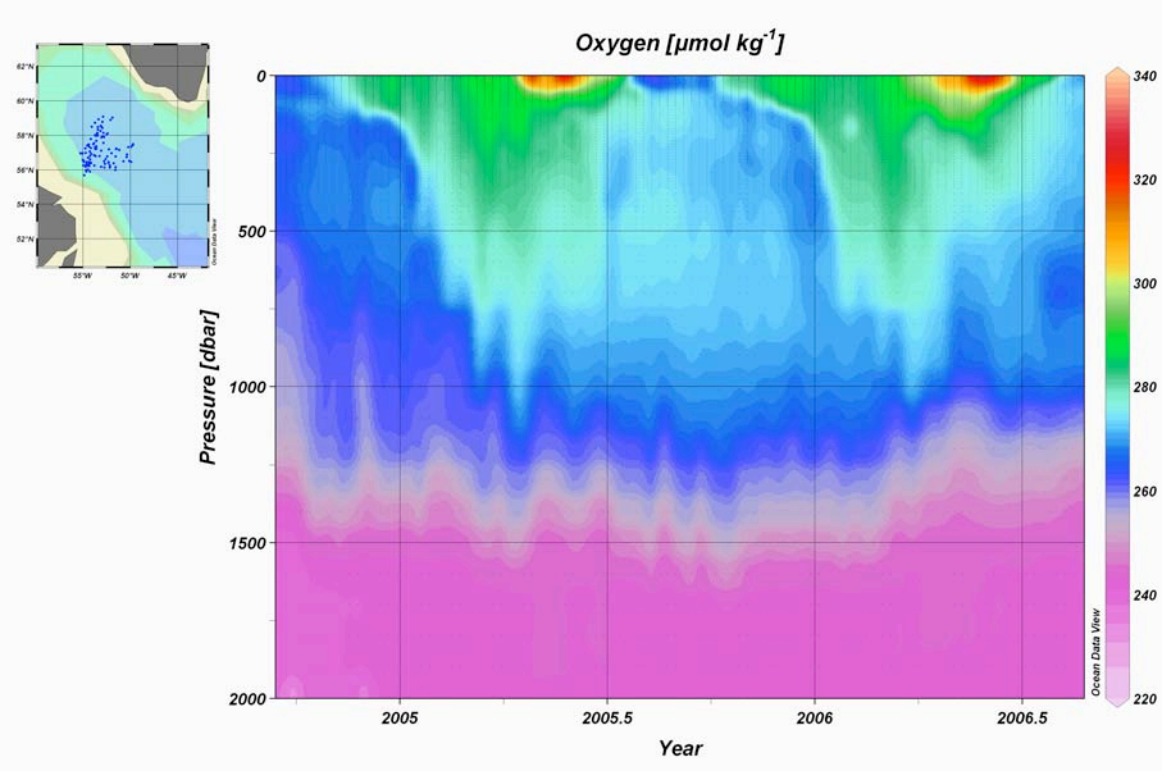

Figure 10: Two-year oxygen time-series documenting two convection periods as measured by a single float that stayed in the central Labrador sea convection region during the entire period (raw oxygen readings, unpublished data, A. Körtzinger and C. Kihm).

4.2 Productivity constraints at Ocean Time-Series Locations

Estimates of the net annual biological oxygen production have been made using monthly measurements of oxygen and carbon at a few ocean time series locations (Table 1). At the Hawaii Ocean Time series (HOT, Fig. 8) these measurements (when scaled to carbon) indicate that the net biological carbon export from the euphotic zone is on the order of 2-3 moles C m^{-2} yr^{-1} (Table 1). This value is larger than predicted for this region by ocean circulation models (e.g., Schlitzer, 2000) and satellite measurements (Laws *et al.*, 2000), both of which depict the subtropical ocean as a region of very little biological activity. A similar situation, in which experimental measurements are greater than model predictions, has been found at the Bermuda Atlantic Time series (BATS, Jenkins and Doney, 2003). The reason for this discrepancy is either that the models and satellite algorithms presently are not sophisticated enough to capture the biological processes in the ocean correctly, or that the experimental estimates from oxygen mass balances are biased due to undersampling.

It is critical to determine the true distribution of biological carbon export so that inventories of this flux and the mechanisms controlling it can be captured in ocean models so that they can accurately predict the response to climate change. It is too expensive to determine annual variations of the concentration of oxygen in the upper ocean in more than a few locations using traditional ship-based measurements. One of the few ways to effectively increase the global distribution of biological oxygen and carbon export estimates is by deploying oxygen sensors on Argo floats. In many ocean locations float speeds are small enough that instruments remain in a general ocean location for more than one year so that the annual cycle of euphotic-zone oxygen concentration can be characterized. Float drift is not

necessarily a problem; if oxygen sensors are deployed on all Argo floats in a given area (e.g. pilot study area), random float movements will cause both emigration and immigration of oxygen floats in the typical 300 km x 300 km Argo square.

Table 1: The annual organic carbon export from the surface ocean determined at three time series locations by different methods. These locations are the time-series stations at BATS (near Bermuda), HOT (near Hawaii), and Station P (in the subarctic Pacific).

	Subtropical Atlantic (BATS)	*Subtropical Pacific (HOT)*	*Subarctic Pacific (Station P)*
		Organic C (mol m^{-2} y^{-1})	
Sediment trap and DOC fluxes	1.8 ± 0.1 [a]	2.4 ± 0.9 [b]	
Oxygen Mass Balance	3.6 ± 0.6 [c]	2.7 ± 1.7 [d] 1.1-1.7 [e]	2.0 ± 1.0 [f]
DIC and $\cdot d^{13}C$ DIC	3.5 ± 0.5 [g]	2.7 ± 1.3 [h] 2.8 ± 0.8 [i]	
^{3}H-^{3}He (OUR)	2.8 ± ?? [j]		

a Carlson *et al*. (1994)
b Benitez-Nelson (2001)
c Spitzer and Jenkins (1989)
d Emerson *et al*., (1997)
e Hamme and Emerson (2006)
f Emerson *et al*., (1991)
g Gruber *et al*., (1998)
h Quay and Stutzman (2002)
i Keeling *et al*., (2004)
j Jenkins and Wallace (1992).

5 Technical aspects: Present status and development needs

5.1 Sensors

To date, two types of dissolved O_2 sensors have been employed on profiling floats. The SBE-IDO (formerly known as the SBE-43) implementation, from SeaBird Electronics, is an electrochemical sensor (Clark cell) (Clark *et al.,* 1953) whose design is similar to the O_2 sensors on SeaBird shipboard CTD units. The Aanderaa Optode is an optical sensor.

The IDO sensor is fully integrated into the SeaBird float CTD system (Fig. 11, left; note that over 90% of Argo floats currently employ a SeaBird CTD system). The Clark cell works on the principle of reduction of molecular O_2 at a gold cathode. In the polarographic mode, the current flow from cathode to anode is proportional to the O_2 concentration of the surrounding fluid. It is usual to cover the electrodes with an oxygen permeable membrane to prevent fouling of the electrodes and to maintain a well-defined chemical medium at the electrode surface. O_2 must diffuse through this membrane in order to reach the cathode and initiate current flow. The Clark cell idea has been around for nearly a century and has been used in shipboard CTD systems since the 1970s. In recent years, SeaBird has made great strides in improving the basic Clark cell arrangement and solving some of the basic problems with this technique. These improvements have been incorporated into the IDO.

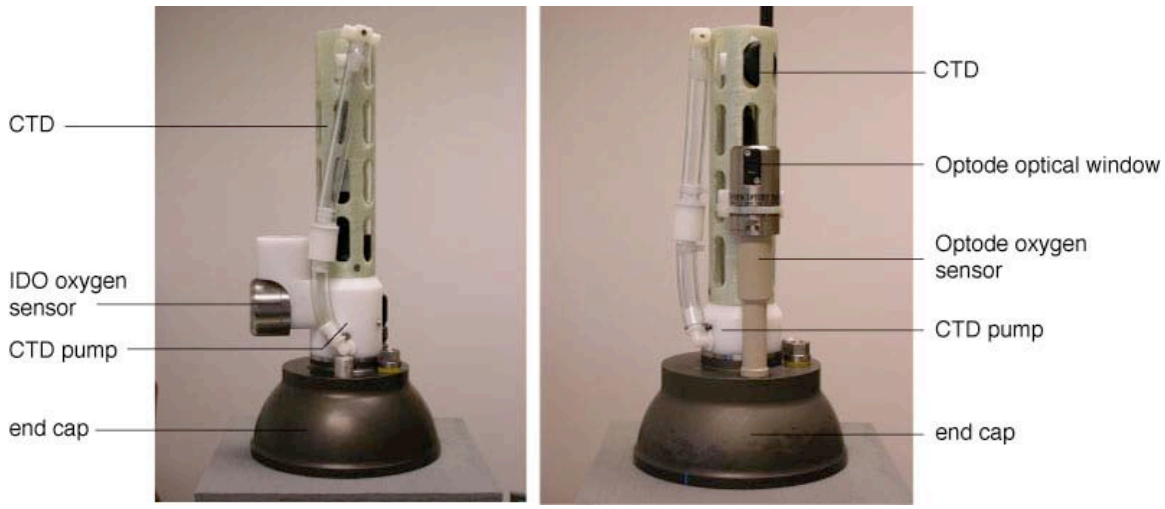

Figure 11a: (Left photo) Upper portion of an APEX float, showing the SeaBird CTD unit and dissolved O_2 sensor. The pump for the unit is contained in the white section located just above the anodized aluminum end cap. The IDO sensor is located in the white section located to the upper left of the pump unit. The temperature and conductivity sensors are located inside the light green plastic mesh. (Right photo) An Aanderaa Optode sensor mounted on an APEX float end cap. The SeaBird CTD is visible behind the Optode. The optical window in the Optode is the dark region centered near the top of the Optode sensor, and the temperature sensor is located just below the window. Because the Optode is not integrated into the CTD unit, it requires a wider end cap than the IDO sensor. (Photos from S. Riser).

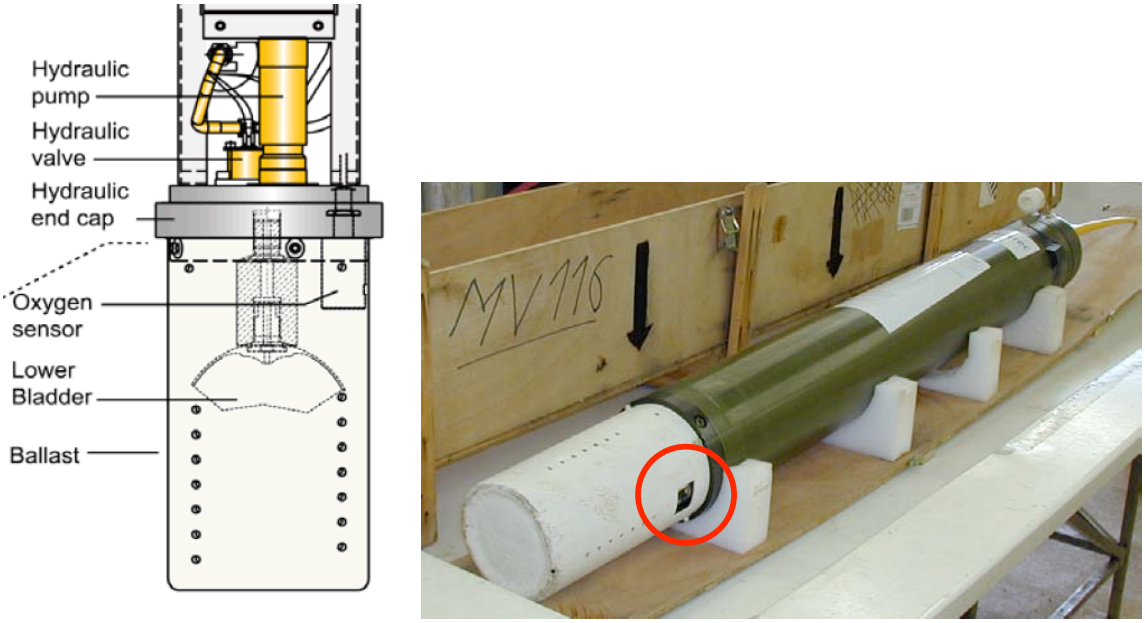

Figure 11b: The lower portion of a PROVOR float, showing the location of the Aanderaa Optode sensor in the float's lower end cap.

For the IDO sensor, seawater is pumped into the fluid circuit and through the temperature, conductivity, and dissolved O_2 sensors, then back out through an exhaust port. Pressure is measured by an external sensor located a few centimeters away (Fig. 11a). Salinity is computed on board the float using the simultaneous measurements of temperature, pressure, and conductivity. The output of the dissolved O_2 sensor is a stream of frequencies, which together with the temperature, computed salinity, and pressure values are transmitted to shore through the satellite data stream. Dissolved O_2 is computed on shore using the transmitted values of temperature, salinity, pressure, and O_2 frequency, in conjunction with a series of calibration coefficients supplied by SeaBird.

The Optode sensor (Fig. 11a, right) operates on the principle of fluorescence quenching (Tengberg *et al.*, 2006). Blue light from a LED in the sensor excites molecules of a fluorescent platinum-porphyrine complex that are immobilized in a film on the sensor optical surface. The excited porphyrine molecules emit photons with a lower energy state (longer wavelength). When oxygen molecules diffuse into the film, they may collide with excited porphyrine molecules before they emit their photons, and energy is transferred to O_2 rather than a loss by fluorescence emission. This reduces the time period (microseconds) over which the fluorescence is emitted by the dye. The sensor operates by detecting the decrease in fluorescence lifetime that is produced by interaction of the dye molecules with oxygen. Detecting changes in fluorescence lifetime, rather than fluorescence intensity, has significant advantages for sensor stability. If some of the fluorescent dye is lost due to photo-bleaching or diffusion from the film, fluorescence intensity will decrease, but the fluorescence lifetime is unchanged.

The values of temperature, salinity, and pressure measured by the SBE CTD are used in the computation of dissolved O_2 on the IDO. The entire CTD/IDO system is integrated, making this computation simple and straightforward. The Optode carries its own temperature sensor; the Optode data transmitted by the float include temperature and frequency/phase information from the output of the sensor. Values of dissolved O_2 are computed on board the sensor but need further pressure and salinity corrections, which are carried out at shore using these transmitted data (alternatively, raw numbers from the sensor can be transmitted to shore and

the entire oxygen calculation can be carried out there; this has some advantages if the calibration coefficients change during the lifetime of the sensor). The algorithm used for inferring dissolved O_2 from the Optode has only a very weak pressure dependency (approx. 4 % decrease in response per 1000 dbar). Since the Optode senses oxygen partial pressure (rather than concentration) by equilibrating the foil material with the ambient seawater, a salinity correction has to be applied to correct for the salinity effect on oxygen solubility in seawater. The manufacturer has made no provision for making measurements of these quantities with the Optode, so values of salinity and pressure from the SeaBird CTD must be used in the Optode O_2 computation.

5.2 Accuracy, Precision, and Response Time

The accuracy and precision requirements for the sensors to meet the scientific goal described above are quite stringent. For accuracy, we determined a threshold of about 5 μmol kg^{-1} and a target of 1 μmol kg^{-1} (*threshold* is the level above which the data are of insufficient quality to address scientific objectives, while the *target* is the desired level of data quality). For precision, we consider a threshold of 2 μmol kg^{-1} as acceptable, while the target precision should be 0.5 μmol kg^{-1}. The long-term drift should not exceed the threshold accuracy. We envision that some of the long-term drift problems can be corrected by combining the oxygen measurements from the floats with independent measurements, taken, for example, from repeat hydrography cruises.

Another issue of importance is the response (equilibration) time of the sensor plus the time it takes for the actual measurement. This total measurement time is a crucial factor, since measurements need to be taken during transit through a vertical oxygen gradient. With a typical ascent speed of 0.1 m s^{-1}, and vertical oxygen gradients up to 3 μmol kg^{-1} m^{-1}, total measurement times (i.e. e-folding times) of considerably more than 10 seconds will result in a smearing-out effect that can lead to errors of a magnitude comparable to the target accuracy of 1 μmol kg^{-1} (Körtzinger *et al.*, 2005). Therefore, total measurement times of less than 10 seconds are preferred, while 30 seconds is about the threshold. For deployments in systems that are characterized by extremly strong vertical gradients in dissolved oxygen (up to 18 μmol kg^{-1} m^{-1}), the required response time would have to be shorter.

5.2.1 Manufacturer's specifications

The manufacturer's stated specifications for several important sensor parameters are summarized in Table 2. The specifications for accuracy and precision are similar for the two sensors. Comparison of these numbers with the threshold and target requirements of the *Argo-oxygen* program reveals that the precision of the sensors is well below the threshold, while the current accuracy level is insufficient. Field and laboratory experience indicate, however, that careful calibration and a few additional changes in the calibration scheme would likely bring the two sensors below the accuracy threshold. For example, with individual foil calibration, Aanderaa was able to demonstrate an accuracy of less than 2 μmol kg^{-1} (see e.g. Tengberg *et al.*, 2006). However, tests by the University of Washington float group showed that this high accuracy is not yet uniformly achieved.

Table 2. Manufacturer's specifications for the IDO and Optode O_2 sensors as for units sold in 2006

Sensor	*Precision*	*Accuracy*	*Stability*	*Sensor Time to Equilibirum*	*Sample Time*
IDO	~1 μmol kg^{-1}	2% of saturation	2% per 1000 hours[c]	12-48 sec[a] <1 sec[b]	2-4 sec
Optode	<1 μmol kg^{-1}	< 8 μmol kg^{-1} or 5% [a]	None given	<25 sec for 63% response (from Aanderaa web site)	8 sec

a: sensor used with a SeaBird 41, with discrete samples;
b: sensor used with a SeaBird 41-CP, with continuous profiling;
c: the 1000 hour figure applies to the time that the sensor is powered-up and in operation, not to the total time of the float mission; in practice, it might require 175-200 profiles to reach this period of time on the SBE 41-CP and many more profiles with the SBE-41.

SeaBird's stated stability of the IDO sensor is just below the threshold stability, largely consistent with experience from field deployments summarized below. Aanderaa lists no standard for stability of their Optode sensor, but the deployed Optodes have shown no evidence of drift over periods of up to 2 years (see below).

In the case of the IDO sensor the equilibration (response) time depends critically on the sampling mode. In a spot-sampled mode (i.e., used with ARGOS data transmission, see below) the sensor must be powered-up and the CTD pump must be running for 12-48 seconds in order to ensure equilibration of the sensor with the in-situ oxygen concentration. For the IDO sensor in a continuous sampled mode (used with the SBE 41-CP on APEX floats with Iridium communications), the 12-48 second interval would apply only at the beginning of the profile, since the equilibration time of a fully powered up sensor is less than 1 second.

The Optode has an e-folding equilibration time of the order of tens of seconds. This relatively long equilibration time is mostly driven by the slow response of the temperature sensor that has been integrated into the Optode. Since the temperature sensor is mounted in a large block of aluminum, it has a large thermal-inertia. This design was chosen since the system was originally developed for deployment on moored systems whose oxygen and temperature concentrations change only slowly with time, so that a slower response system resulted in a better precision. The actual response time of the Optode is substantially faster. Therefore, this problem has been partially circumnavigated by using the temperature measurement from the float to recompute the oxygen concentration (although the Optode is calibrated using its native temperature, not the float sensor, a potential problem). In the longer run, a temperature sensor with a faster response time needs to be integrated into the Optode system. Even by itself, the Optode has a longer equilibration time than the IDO. This is because the optical film in the Optode must be thick enough to ensure that sufficient porphyrine molecules are available to provide the fluorescent signal. The equilibration time of the Optode is a relatively strong function of temperature and pressure, so that it takes considerably longer to equilibrate the sensor in deep waters compared to near-surface waters. There also appears to be a difference in the response time between a positive and a negative oxygen gradient.

Once equilibrated, the sampling time of the two sensors are very comparable, about 2-4 seconds for the IDO and about 8 seconds for the Optode. This corresponds to a depth interval

of less than 1 meter, which is generally fast enough to eliminate the possibility of biases due to vertical smearing, even in regions of strong vertical gradients.

5.2.2 Field experience

Experience has shown that the specifications by the manufacturers are accurate in a number of cases, but in others cases, sensors of both types have not met these standards. The determination of the accuracy, precision, and long-term stability of field-deployed dissolved oxygen sensors is somewhat limited. For example, one major difficulty that we have had to face in doing at-sea calibrations of oxygen floats is the 10-day gap between the ship-based Winkler titrations (performed on the same day as the float deployment) and the first float oxygen profile (this difficulty was overcome in 2006, with floats now available that can make their first profile immediately after sinking to their parking depth). Often, in addition to the 10-day interval, the float may have drifted several tens of kilometers away from its launch site, making the comparisons between Winkler data and the data from the floats less than ideal.

In what follows next, we show a few representative examples from floats with single sensors as well as results from a few floats where both sensors were mounted. A more complete description of the field experience by various groups is given in the appendices.

IDO Sensor:

Experience with the IDO sensor has been generally positive. For example, an IDO-equipped APEX float near Hawaii showed very little sensor drift over 3 years both near the sea surface and at 2000 m, albeit with a significant offset relative to independent in-situ determinations of the dissolved oxygen content by Winkler titrations of bottle samples (Fig. 12).

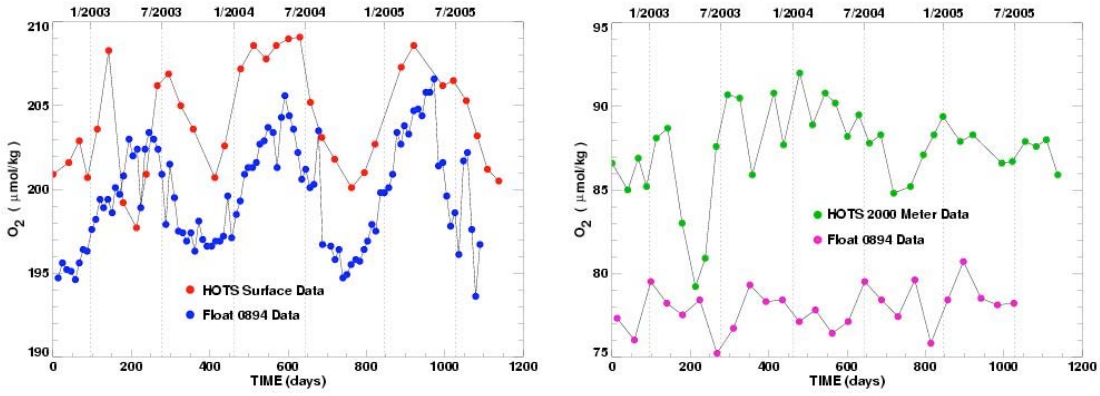

Figure 12. (Left panel) Near-surface dissolved O_2 as measured by an IDO equipped float (WMO 4900093, University of Washington float group) near Hawaii during the period 8/2002 through 9/2005, shown with accompanying shipboard-based bottle samples analyzed by the Winkler method by the Hawaii Ocean Time Series (HOT) program. (Right panel) As left panel, but for 2000 m. Note that in both cases there is little evidence of long-term drift over the course of 3 years, although there is in both cases a systematic offset between the float measurements and the Winkler-derived sample values. (From S. Riser.)

For the near-surface samples, the IDO is typically about 5 µmol kg^{-1} below the Winkler values, or about 2.5% low. This is approximately consistent with the manufacturer's

specification for accuracy, but just at the threshold accuracy desired. Several IDO sensors, however, have exhibited long-term drift that is well outside the acceptable level (Fig. 13).

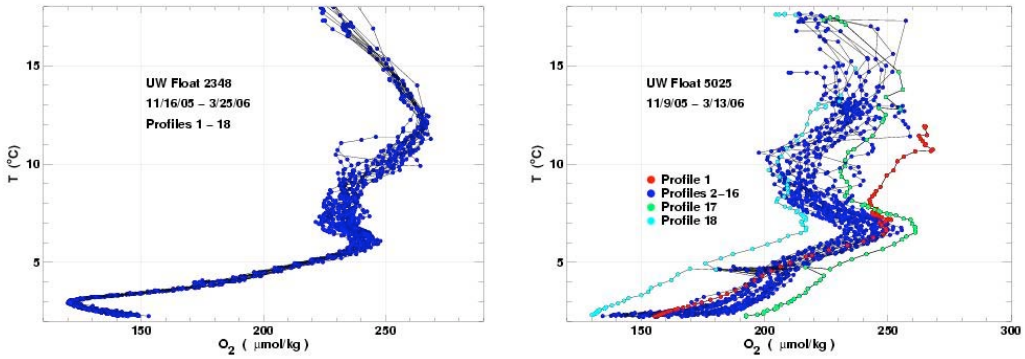

Figure 13. (Left panel) Temperature-oxygen relation from UW Argo float 2348, equipped with an IDO sensor, from 18 profiles during the period 11/05 through 3/06. The float was located near 40°S in the eastern S. Pacific. Note the high degree of repeatability in the T/O_2 relation, indicating high sensor stability over this period. (Right panel) A similar diagram using data from UW float 5025, also from the eastern S. Pacific. Note the jumps in the T/O_2 relation, indicating episodic drift of the IDO sensor. The causes of such jumps are presently under investigation. (From S. Riser.)

In the case of float 5025 (Fig 13, right panel) it is obvious that the IDO sensor is drifting badly over the entire water column. Of the approximately 35 floats equipped with IDO sensors deployed to date by the University of Washington Float Group (UW), about 15% have shown behavior similar to float 5025 It is speculated that the jumps are related to small tears in the membrane inside the Clark cell that occurred during float ballasting operations or shipping. SeaBird has recently made important progress in correcting this problem, and IDO sensors on floats recently deployed have not shown this problem.

Optode Sensor:

Experience with the Optode also has been quite positive, particularly for deployments at higher latitudes. Gilbert *et al.* (pers. comm.) found differences of less than 5 μmol kg^{-1} between float data and bottle oxygen titration data in their deployment of an Optode-equipped float in the Labrador Sea (Fig. 14a, b). These differences are below the threshold accuracy, particularly if one takes into account that the float measured the water column 10 days after the deployment.

By contrast, the agreement of the Optode measured dissolved oxygen concentration and those determined by shipboard Winkler titration of water samples were substantially worse for a similar float deployed in the Gulf of Alaska (Fig. 14c, d). In other examples from the Labrador Sea, major calibration offsets relative to Winkler data have been identified that greatly exceeded accuracy claims made by the manufacturer (e.g. Körtzinger *et al.*, 2005). These appear to be due to problems with the calibration procedure performed by the manufacturer. Major efforts are currently underway to solve this problem.

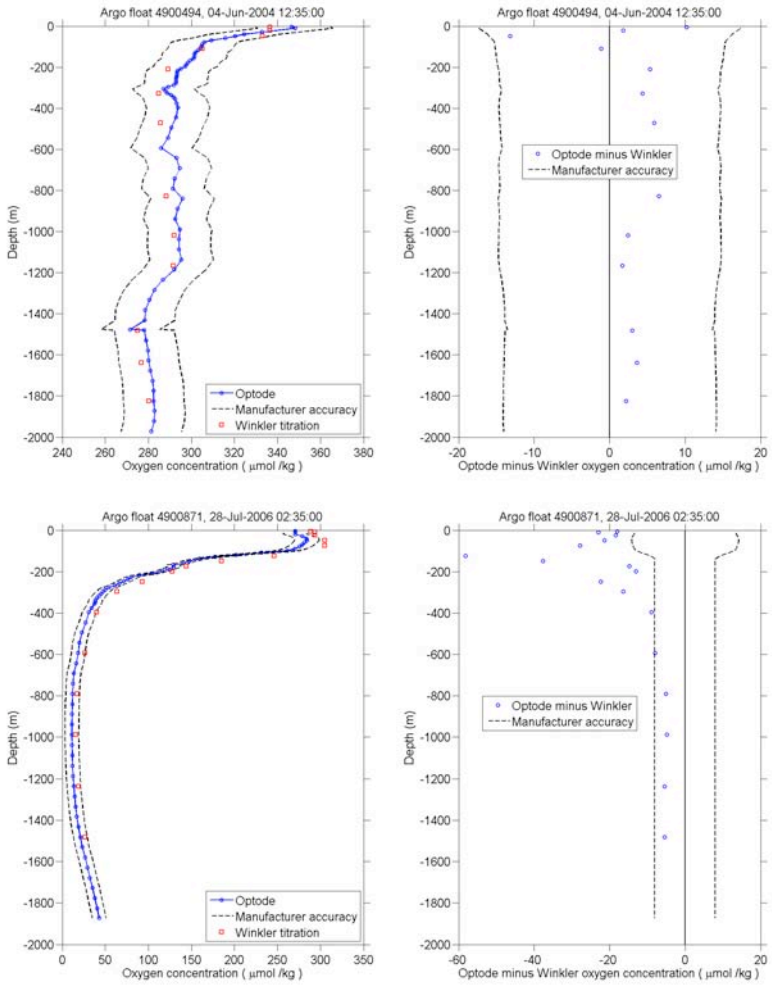

Figure 14: At-sea comparison of optode and Winkler bottle oxygen titration data for deployments in two different oceanic regimes. (a) and (b) Comparison for float 4900494 deployed in the Labrador Sea. (c) and (d) Comparison for float 4900871 deployed in the Gulf of Alaska. While the Optode performs well in the Labrador Sea, substantial differences are found in the Gulf of Alaska, reflecting perhaps, differences in temperature and vertical oxygen gradients. The manufacturer accuracy is 8 _mol kg^{-1} or 5%, whichever is greater. Data from D. Gilbert. The Optode measurements reported here are those computed using the Optode's temperature sensor.

The results suggest that the Optode performs better in conditions of weak vertical temperature and oxygen gradients, probably due to its slow response time. As many of these slow response problems seem to stem from the slow response of the temperature sensor integrated into the Optode system, they can be at least partially addressed by recomputing the O_2 concentrations using the CTD's temperature sensor. This was not done in the examples shown here, however.

One important strength of the Optode is that nearly all deployments to date suggest a very high degree of long-term stability. Both Körtzinger *et al.* (2005) and Gilbert *et al.* (2005) show long term stability of Optodes over times as long as 2 years from several sites in the world ocean (Fig. 15).

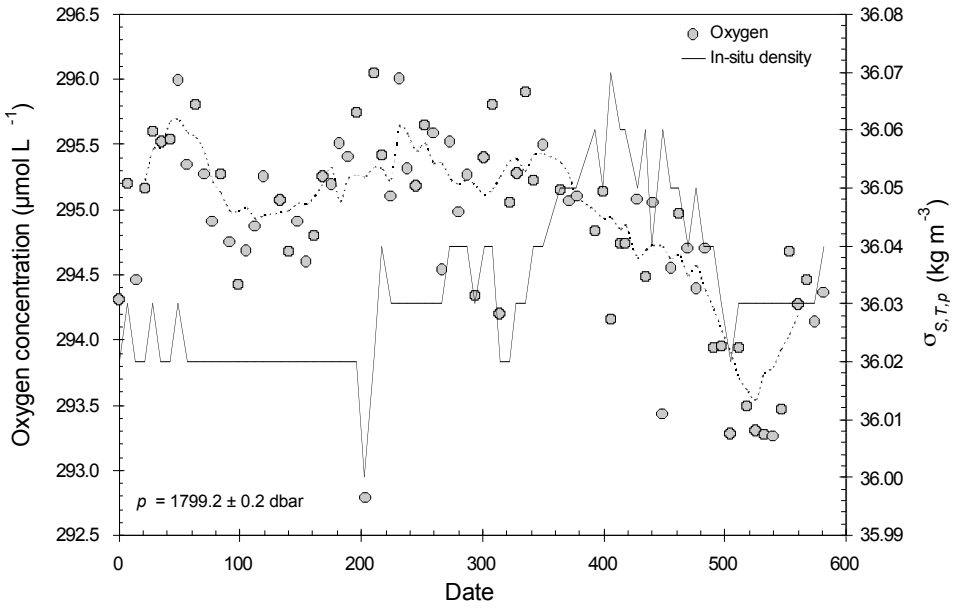

Figure 15. Oxygen and density data at a depth of 1800 m collected during 580 days by an APEX float in the Labrador Sea... In the central Labrador Sea (the first 400 days), it is expected that measured salinity, temperature and oxygen values at this depth should be rather constant. The data demonstrate no drift over the given time period, but as the float moves out of the Labrador Current the measured oxygen and density values shift slightly. The average measured oxygen during the entire period was 295.0 ± 0.7 μmol L^{-1}. The dotted line is a 7-point centered running mean of the measured oxygen concentrations (from Tengberg *et al*., 2006).

It should be pointed out that the Optode sensor is capable of measuring oxygen in (moist) air. If mounted on the float's upper end cap, oxygen measurements can be performed while the float is at the surface during data transmission. If sea-level barometric pressure at the place and time of the floats surfacing can be inferred from other sources (e.g. from re-analysis products), the oxygen reading in air can be predicted (Körtzinger *et al*., 2005). and used as a simple drift check.

Floats with both IDO and Optode sensors:

In order to investigate the relative merits of the IDO and Optode sensors, several UW floats have been deployed carrying both sensors. One such float was deployed near the Hawaii Ocean Time Series (HOT) site northeast of Hawaii (Fig. 16).

The measured O_2 from the Optode and the IDO are similar in the deep water, below about 700 m (Fig. 16, middle plot, green line). This agreement is heartening: the measurements from two independent sensors, using two completely different technologies, agree to within 2 µmol kg^{-1} over the deepest 1300 m of the profile [note the dark green line in the middle plot, showing ΔO, defined as O_2 (Optode) minus O_2 (IDO)]. Above about 600 m, however, the measured values from the two sensors depart markedly, with the differences increasing at shallower depths. In general, the values of O_2 measured by the Optode are as much as 10 µmol kg^{-1} above those measured by the IDO. In this case it is known that the IDO values are near to correct, since the surface saturation as measured by the IDO is near 101% (in agreement with concomitant Winkler samples), while that measured by the Optode is closer to about 110%, clearly too high for the surface saturation value at any time during the year (these differences were seen over profiles throughout the annual cycle, as can be seen at *http://flux.ocean.washington.edu/argo/homographs/0035.html*).

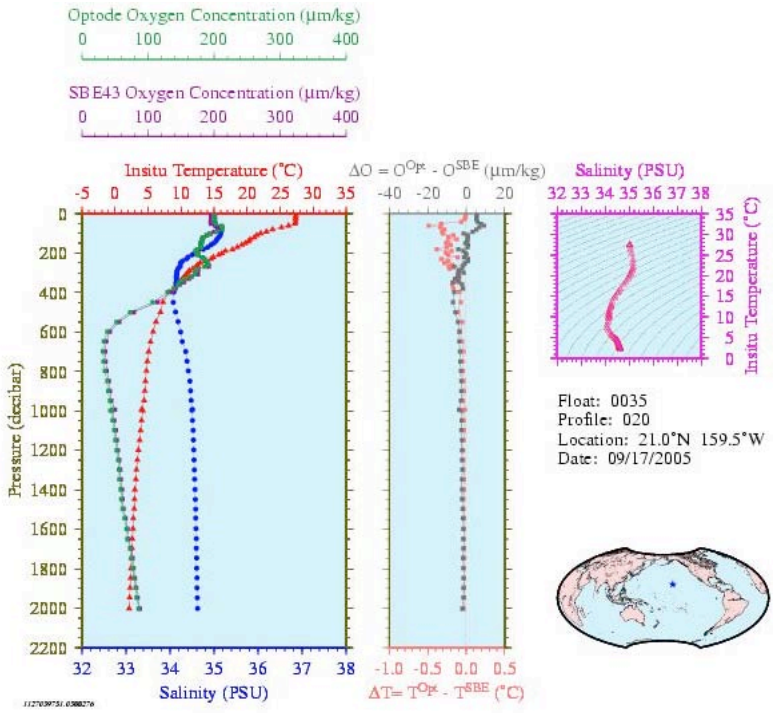

Figure 16. (Left panel) Temperature, salinity, and dissolved O_2 from UW float 0035, near the HOT site at Hawaii. The dissolved O_2 is shown for both the IDO and Optode sensors. (Middle panel) The difference in dissolved O_2 between the Optode and IDO sensors (green line) and the difference in measured temperature between the Optode and the SeaBird CTD (pink line). (From S. Riser.)

Part of the reason for this difference appears to be that the temperature measured by the Optode, and used in the Optode oxygen calculation, is incorrect by as much as –0.8 °C (Fig. 16, middle plot, pink line). In the deeper waters (below about 700 m), where the vertical temperature gradient is relatively weak, the Optode and IDO agree well in both temperature and dissolved O_2. At shallower levels, however, in the main thermocline, the Optode temperature is consistently too low – a result of the slow response time of the temperature sensor. With the Optode temperature too low, the inferred O_2 is generally too high (Fig. 15). Other situations where the Optode O_2 is much too low also occur in the presence of steep vertical gradients (Fig. 14). Körtzinger *et al*. (2005) remarked on a similar slow response to the Optode thermistor in their Labrador Sea results, although the vertical temperature gradient at these higher latitudes tended to be somewhat less than the thermocline gradients at the HOT site.

Comparison of the oxygen data from several more floats that carry both oxygen sensor types reveal a complex behavior to the sensor differences (Fig. 17). Above about 500 m, where the vertical temperature gradients are largest, the two oxygen measurements differ due to the thermal inertia of the Optode temperature measurement, as discussed previously. However, the result of this erroneous temperature measurement can be Optode O_2 values that are apparently *either too high or too low*. In all cases shown here the vertical temperature gradient was positive since the floats were all equatorward of 32°N, so that the impact of these errors seem to be sensor-dependent. In summary, it appears as if the near-surface measured differences between sensors are primarily due to Optode errors. This conclusion is supported by a series of sensor tests executed at the Float Group of the University of Washington and summarized in the appendix.

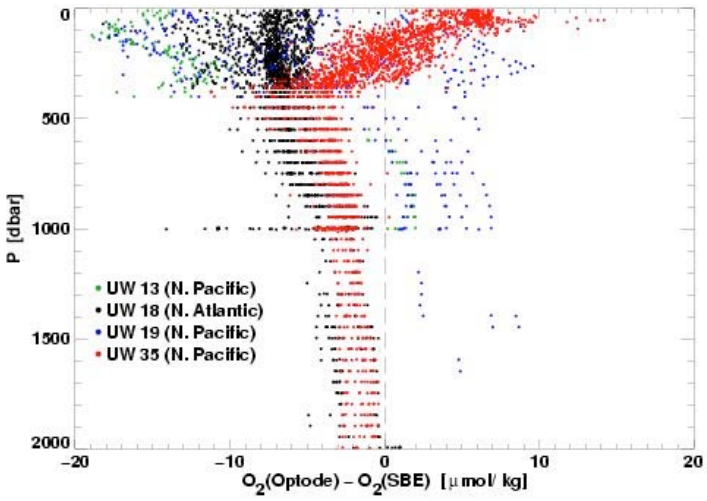

Figure 17: The difference between Optode measured O_2 and IDO O_2 as a function of pressure for 4 UW floats deployed in the Atlantic and Pacific Oceans. All floats were deployed equatorward of 32°. Note the variation of the differences with pressure: at relatively high pressure (low temperature) the Optode shows values less than the IDO sensor, while about 500 m, in the thermocline, the Optode measurements can be either higher or lower than the IDO. (From S. Riser.)

5.2.3 Assessment of current accuracy, precision, and response time of the sensors

The analyses undertaken so far reveal strengths and weaknesses of the two sensors in terms of accuracy, precision, long-term stability, and response time. The advantages of the Optode sensor appear to be its excellent long-term stability and high precision. It also appears to be accurate provided that it has sufficient time to come into equilibrium with the surrounding temperature and oxygen concentration and provided that its temperature response has been carefully calibrated (possibly by individual sensor factory-calibration plus in-situ calibration check/correction based on concomitant Winkler profile, see Appendix 9.1). The main disadvantage of the Optode sensor is its relatively slow response time, which tends to lead to problems in the upper ocean, where vertical gradients in dissolved oxygen and temperature are greatest. The advantage of the IDO is its high precision and its faster response time. It tends to be somewhat less accurate than the Optode sensor and also tends to have higher drift.

Relative to the threshold and target specifications of the program, both sensors do well with regard to precision, but improvements are needed in terms of accuracy and long-term stability for both sensors. For the Optode, improvements in its response time behavior are also needed. Specific recommendations are given in section 5.8.

The performance of the sensors in extreme environments, such as anoxic zones, has not yet been well established. This is in part due to the fact that the standard Winkler method is not accurate at very low O_2 concetrations (< 20 μmol kg^{-1}), with special low-oxygen analysis techniques required in such regimes. Fundamentally, the Optode appears to be slightly superior in such systems, since it is less sensitive to potential interference from reduced species, such as H_2S.

This assessment is based on the current generation of sensors. However, both companies are currently in the process of improving their sensors. Nevertheless, the high levels of accuracy

and precision needed to address some of the scientific questions outlined above will likely require additional careful testing and calibration of the sensors before deployment of these sensors in large numbers is undertaken, and significant post-processing of the data will likely be required.

5.3 Communications

Since the mid-1980s, when profiling floats first came into use, the ARGOS (not to be confused with the Argo Project) satellite system has been used by nearly all profiling floats for transmitting data from the float to shore-based analysis stations. The ARGOS system has been quite reliable but suffers from very low effective data throughput (< 1 baud) and relatively high cost in some countries. In recent years a number of floats have been tested that use the Iridium satellite system for communication, and this has so far worked very well. At present, the Iridium system has some advantages over ARGOS because (1) the data throughput is much higher, on the order of 2400 baud; (2) the cost per profile is comparable to ARGOS in many countries and considerably less in others; and (3) the ability for real time, 2-way communication with the floats exists with Iridium, whereas for ARGOS this is presently not possible. The next generation ARGOS program (ARGOS-3) (see *https://www.argos-system.org/html/system/enhancements_en.html*) was launched in October 2006, promising 2-way communication and 10 times higher data throughput. However, no experience has been gained so far with this system. On the other hand, ARGOS has at least one strong advantage over Iridium: it has been a stable organization for 3 decades, while Iridium suffered bankruptcy in 1998. At this time approximately 60 Iridium floats have been deployed by the UW Float Group, with these numbers likely to increase in the next few years. The Iridium implementation developed at UW for APEX floats is now commercially available through Webb Research, and a number of countries participating in Argo have expressed interest in ordering Iridium floats in the near future.

The higher data rate possible with Iridium means that much more data can be sent for each float profile, even while the float transmits on the surface of the ocean over a much shorter time than is necessary with ARGOS. For floats using ARGOS, it is typical that a CTD profile consisting of 71 temperature-salinity pairs between 0 and 2000 m, plus a small amount of engineering data, requires 9-15 hours of transmission time at the sea surface. The transmission time depends on the latitude of the float, with floats at low latitudes requiring longer transmission times (this is because ARGOS has only 5 satellites in its constellation). On the other hand, for floats equipped with Iridium, a profile consisting of 1000 temperature-salinity pairs between 0 and 2000 m (i.e., data reported at 2 m intervals) requires only about 7 minutes of transmission time on the sea surface, and the possibility exists to send information back to the float to alter its mission.

The number of samples that are taken during a profile impacts how the CTD pump is operated. For an APEX float that uses ARGOS communication and hence samples only at 71 depths, the CTD pump is turned on for a few seconds while a sample is collected and then turned off until the next sample. Since the samples are usually at least 4 m apart (and as much as 100 m apart in the deepest part of the profile), this is a sensible strategy to collect data and save energy, especially since the float will later use a great deal of energy for transmitting the data over a long period at the surface. For an APEX float that uses Iridium communication and hence can sample many more depths, the CTD pump is turned on at the bottom of the profile and left on for the entire profile, since samples will be collected at very close depth

intervals. This requires considerably more energy than in the ARGOS case, but since the float transmits on the surface for only 5-10 minutes, much less energy is consumed by the float in the data transmission process. Overall, the total energy required for one profile (pumping + data transmission) is slightly higher for Iridium-equipped floats.

5.4 Sensor-CTD integration and operation

Two types of floats have been used in significant numbers in Argo. Approximately 65% of the Argo array consists of APEX floats, with 30% of the array made up of SOLO floats. Nearly all oxygen sensors deployed to date have been installed on APEX floats, and the discussion that follows here is based on experiences with sensors on APEX floats only. Due to the widely differing data transfer rates of ARGOS and Iridium, and the resulting differences in CTD pump operation, different configurations are possible.

In the case of ARGOS communication, the CTD used is a standard SeaBird Electronics SBE-41. This is a CTD unit specially configured for use on profiling floats and has been widely used by the float community since 1997. When Iridium is used for communication, and the CTD pump is turned on and left on, the CTD used is the SBE-41 CP (CP: continuous profiling). The hardware for these two CTD versions is nearly identical, but there are differences in the controlling software. Thus, for O_2 measurements on APEX floats, there are 4 possible combinations of sensors and CTD units, with advantages and disadvantages to each. Each of these possibilities is discussed here:

(*i*) IDO on an ARGOS float (i.e, SBE-41 CTD): Here, O_2 is spot sampled at each of the 71 points from 0-2000 m. Since the response time of the IDO sensor is 12-48 seconds (Table 1), the CTD pump must be left on for this amount of time for each O_2 sample. For *T*/*S* sampling alone, without dissolved O_2, the CTD pump must only be on for about 2.5 seconds. Thus, adding dissolved O_2 to ARGOS floats is a costly proposition in terms of the amount of energy required per sample, and it is likely that the number of profiles collected by a float over its lifetime will be significantly less than for instruments that collect T and S only (i.e., a standard Argo float). With this in mind, the Argo community is likely to be less than enthusiastic about adding IDO sensors to ARGOS-equipped floats.

(*ii*) IDO on an Iridium float (i.e., SBE-41 CP CTD): In this case the CTD pump is turned on at the beginning of the profile (i.e., 2000 m) and left on during the entire ascent phase of the float. Since the pump is running continuously, and since the O_2 sensor by itself consumes very little energy, an IDO/Iridium float consumes nearly the same amount of energy as an Iridium float with T/S sampling only; in this case the addition of O_2 appears to be not very costly, from an energy standpoint, a potentially strong selling point to the Argo community. The first float of this type has recently been deployed near Hawaii. SeaBird has recently redesigned its controller board layout and added a more efficient CTD pumping motor, and thus it is likely that the lifetimes of floats using a 41-CP CTD will increase in the near future, whether they employ oxygen sensors or not.

(*iii*) Optode on an ARGOS float (i.e., SBE-41 CTD): This situation is nearly opposite to case (*i*) above. The CTD pump is turned on for a few seconds at each of the 71 levels where data are collected. During this time the drain on the batteries is quite high, with currents of up to 30 mA flowing while the pump is on. On the other hand, the Optode (which is not connected to the CTD) requires only a few milliamps to collect a single sample, which can be carried

out during the time the CTD data are being collected. Thus, the addition of an Optode to an Argos float with SBE-41 CTD requires a relatively small amount of additional energy.

(*iv*) Optode on an Iridium float (SBE-41 CP CTD): This situation is the mirror-image of case (*ii*) above. The CTD pump is already on continuously for the entire profile, with T and S samples being collected at 2 m intervals. To sample the dissolved O_2 using an Optode at the same rate, the few mA required for each O_2 sample would have be repeated 1000 times for a 2000 m profile, a substantial use of battery power. Thus, this is unlikely an attractive option for floats in the Argo project. However, it is certainly possible to collect oxygen data at lower resolution (at the same resolution as with ARGOS, for example), in which case the combination of Iridium/Optode is just as attractive from an energy standpoint as Iridium/IDO, although without the additional resolution.

With the possible advent of ARGOS-3, additional configurations are possible, but have not yet been tested.

5.5 Energy Consumption and Implications for Float Lifetime

The actual increase in energy required to operate a dissolved O_2 sensor in the four APEX cases discussed above (compared to standard T/S floats) has been measured recently at the UW Float Lab using floats that were under pressure in a pressure vessel. Using this information, the maximum number of profiles and the maximum float lifetime has been estimated (Table 3), assuming that profiles are collected at 10-day intervals and assuming that floats will fail due to dead batteries. Other failure modes exist of course, but there are no known float failure modes associated with the addition of O_2 sensors. In addition, it is assumed that the floats are equipped with 3 lithium battery packs. There is now a large body of evidence that suggests that the alkaline battery packs used in most APEX floats prior to 2004 have a high probability of premature failure due to high current drain on the batteries when the buoyancy pump is turned on. For this reason, many APEX groups have now switched to using lithium batteries. While there is a moderate added expense with lithium batteries and additional logistical problems associated with their use, their use has been shown to increase APEX float lifetimes significantly. Our assumption is also consistent with the recent recommendation of the Argo Science Team that all groups in Argo consider switching from alkaline to lithium. When estimating the number of profiles and hence float lifetime in Table 3, the battery lifetimes were suitably derated for self-discharge effects.

Table 3 reveals that the addition of dissolved oxygen sensors will reduce the float lifetime by between 10% to 30%, depending on the exact configuration. This is a modest reduction but needs to be considered when calculating the cost of the *Argo-Oxygen* program. If the addition of the oxygen sensor is combined with the use of the more efficient SBE CTD pump (announced by SeaBird and to be implemented in mid-2007), the extra energy cost of the oxygen sensor can be compensated, leading to virtually no change in the float life time relative to the currently used APEX/Iridium float with the SBE-41 CP.

Table 3: Estimates of float lifetimes for various sensor configurations, with and without O_2 sensors, based on UW laboratory measurements on floats under pressure. It is assumed that each float carries 3 lithium battery packs (each with 4 DD cells) and that the floats are parked at 1000 m and profile to 2000 m on each profile. The estimates have been downrated for battery self-discharge.

Float type/mission	*O_2-sensor*	*Number of T/S samples*	*Number of O_2 samples*	*Number of profiles possible*	*Duration @ 10 day sampling (years)*	*Reduction relative to T/S only*
APEX/ARGOS	–	71	0	288	7.9	–
APEX/ARGOS	Optode	71	71	254	6.9	-13%
APEX/ARGOS	IDO	71	71	190	5.2	-34%
APEX/Iridium	–	1000	0	257	7.0	–
APEX/Iridium	Optode	1000	71	227	6.2	-11%
APEX/Iridium	IDO	1000	1000	219	6.0	-14%

5.6 Current costs estimates

The costs of the proposed Argo-Oxygen program arise from the sum of several components. The following elements need to be considered: (i) costs of the oxygen sensors, (ii) costs for adding the sensors to the floats, (iii) costs for testing or calibrating the sensors, (iv) costs affecting the float lifetime from any increased energy demand from sensor operation, float operation, or increased data transmission requirements, (v) telecommunications costs, (vi) costs for data handling, and (vii) costs for data quality control. These costs have to be compared to the costs associated with a standard Argo float that measures temperature and salinity only.

In estimating these costs, it needs to be considered that, so far, nearly all deployments of Argo floats with oxygen sensors were done on an opportunity basis, often bootlegging on other programs. Therefore, the cost estimates arising from these deployments vary quite considerably between the various groups. The costs reported here are mostly based on the experience of the UW Float Group.

Table 4 reports the costs associated with items (i)-(iii) and (v), not including those associated with items (iv) and (vi)-(vii). Those are shown in Table 5. Inspection of Table 4 reveals that the addition of oxygen sensors to ARGO floats can increase the cost of an individual float by 20-30% compared to the cost of floats without O_2 sensors. Most of the additional cost is due to the cost of the sensors themselves, although substantial additional pre-deployment preparation costs and experienced technical personnel in float laboratories will be required for the foreseeable future for both types of sensors. We note that it is possible to purchase floats with both types of O_2 sensors in a ready-to-deploy configuration directly from the float manufacturer; however, experience has shown that at this time the quality of O_2 data derived from such floats is not generally within the sensor manufacturer's stated specifications. In the future, it is possible that these additional preparation costs will decrease or disappear altogether, as the batch-to-batch quality of the sensors improves.

Table 4: Estimates of the 5-year cost of fabricating and deploying Argo floats with and without O_2 sensors. All costs in the table are given in US$ and all prices are based on typical costs in the US.

Float/Comm. Type	*Float Hardware*	*O_2 Sensor Type*	*Sensor*	*Sensor Prep.*[a]	*5-Year Comm.*[b]	*Total 5-Year Cost*	*Change Relative to T/S*
APEX/ARGOS	14000	–	0	0	1800	15800	
APEX/ARGOS	14000	Optode	3800	400	2300	20500	+30%
APEX/ARGOS	14000	IDO	2800	100	2300	19200	+22%
APEX/Iridium	16000	–	0	0	1530	17530	
APEX/Iridium	16000	Optode	3800	400	1600	21800	+24%
APEX/Iridium	16000	IDO	2800	100	2000	20900	+19%

NOTES:
a:The sensor preparation costs include calibration (Optodes) and check against a known standard (IDO).
b: The communications expenses are estimated by assuming a cost of US$10 for a standard ARGOS profile with temperature and salinity only (the cost in the US is slightly lower than this; in many countries it is somewhat higher). The Iridium costs are estimated at $8.50 per profile for GPS and temperature/salinity only, approximately the present UW cost. This cost might vary from user-to-user and country- to-country. The Iridium/Optode float communications costs are estimated assuming that 71 O_2 samples were collected during a high-resolution T/S profile. The additional cost for the transmission of the oxygen data was based on the estimated relative increase in data transmission, i.e. about 30% for ARGOS/Optode, ARGOS/IDO, and Iridium/IDO, whereas the marginal costs for the Iridium/Optode are very small, since only 71 additional samples are transmitted relative to 1000 for T/S, hence only an increase of about 5%.

The total estimated cost per float per 5 years of the *Argo-Oxygen* program is shown in Table 5. This table has been constructed by combining information from Table 4 with the reduction in lifetime estimated in Table 3. In addition, we estimated about US$200 per float per year in additional cost for data handling and quality control. The latter is substantially more than currently budgeted for T/S, but we envision that the quality control for dissolved oxygen entails substantially more effort than needed for T/S. For example, in order to produce research quality data, the quality control will likely require a secondary quality control step, where each profile is checked against expected values stemming from a climatology. This cost will likely decrease with time as the sensors improve and the quality control procedures become more standardized.

The total estimated 5-year cost per float of the *Argo-Oxygen* program above the core Argo mission comes to about US$6500 to US$9200, or about US$1300 to US$1840 per float and year. With a profile every 10 days, the per profile cost amounts to between US$36 and US$50. Assuming 71 samples per profile, this equates to US$0.50 to US$0.71 per oxygen sample. If we disregard the APEX/ARGOS/IDO option, which is particularly expensive due to its substantial reduction in float lifetime, this represents an increase of roughly 40% relative to the cost of operating the core mission of Argo. This cost estimate is relatively insensitive to the exact configuration, as it varies only between 37% and 47%.

Table 5: Estimates of the total 5-year cost of adding oxygen measurements to Argo on a per float basis. Shown are the marginal costs only, i.e. those above the operation of the core Argo program. All costs in the table are given in US$ and all prices are based on typical costs in the US.

Configuration (APEX float)	*O_2 Sensor[a] (i)*	*Sensor Prep.[a] (ii) & (iii)*	*5-Year Comm.[a] (v)*	*Incremental Cost From Reduced Float Lifetime[b] (iv)*	*Data Handling & Control[c] (vi) & (vii)*	*Total Estimated Cost Per Float*	*Change In Cost Relative To T/S[d]*
ARGOS/Optode	3800	400	500	1800	1000	7500	+47%
ARGOS/IDO	2800	100	500	4800	1000	9200	+58%
Iridium/Optode	3800	400	70	1800	1000	7070	+40%
Iridium/IDO	2800	100	470	2200	1000	6570	+37%

NOTES:
a: From Table 4
b: Estimated from the relative reduction of the float life-time given in Table 3 and the total purchase cost of an APEX T/S float given in Table 4, i.e. US$14,000 for an APEX/ARGOS float and US$16,000 for an APEX/Iridium float.
c: Estimate based on experience with quality control for salinity.
d: Relative to the total 5 year operation cost of an APEX T/S float, i.e. US$15,800 for an APEX/ARGOS float and US$17,530 for an APEX/Iridium float.

A substantial fraction of the costs are associated with the impact of the O_2 measurements on the float lifetime. Therefore a minimization of this impact, by investing into the use of a high efficiency CTD pump, is very attractive. We currently do not have sufficient information at hand to assess the total cost reduction of such an action, but floats in this configuration will be built and deployed later in 2007, and an assessment of this issue should be possible soon.

5.7 Summary and conclusions

In conclusion, the technology for an *Argo-Oxygen* program is nearly ready, but several problems with the sensors and their integration with CTD units need to be solved before a full-scale deployment is justifiable:

(1) It appears from the work of Körtzinger *et al*. (2005) that the Optode is generally stable over times of 1-2 years, based on a number of measurements of this duration. The IDO has been found to be less stable (i.e., more sensor drift) in some cases, although in others (e.g. float WMO 4900093) the IDO has shown remarkable stability over more than 3 years.
(2) The initial calibration on the IDO would appear to be better in general than that on the Optode, largely because only a small fraction of all Optode sensors are actually calibrated at the factory (the calibration results from a few sensors in each batch are averaged and then applied to the entire batch).
(3) There appears to be a temperature-dependent error in the calibration of the Optode (partially caused by a thermal mass error in the Optode temperature sensor), and possibly a pressure-dependent error in the calibration of the IDO. In both cases the manufacturers are examining these problems and attempting to remedy them.

(4) There is an interaction between CTD pump operation, energy demand from the dissolved oxygen sensor, and the speed of the chosen communication system. The APEX/Iridium/IDO system seems to be advantageous, since it permits for the measurement of ten times more samples without having a higher impact on the reduction of the float lifetime

The good news is that the problems noted here, while not unimportant, should be solvable in the near-term. In each case a reasonable hypothesis exists for the cause of the problem, and potential remedies are being tested. It seems likely that in a very few years it should be practical to consider the possibility of making long-term, high quality measurements of O_2 from a large number of profiling floats.

5.8 Recommended Action Items for the near-term

We recommend that the following action items be implemented as soon as possible:

(1) *Continue Sensor development*: SeaBird has already made great strides with the Clark cell sensor, and they should be encouraged to continue to improve this technology by studying the drift characteristics of their IDO and eliminating this problem. Aanderaa should be encouraged to improve the response time of their sensor, both with regard to temperature and dissolved oxygen concentration.

(2) *Improve Calibration*: The manufacturers should be encouraged to redouble their efforts at understanding the calibration problems and provide remedies as soon as possible. Once floats are deployed, they will continue to provide data for >5 years (hopefully). Whatever errors are present in their sensors upon deployment will remain for the life of the float. Thus, it is imperative that fixes to these problems be found quickly, as there will be a reluctance to deploy O_2 floats in large numbers before these deficiencies are addressed. In addition to the general understanding of the temperature and pressure effects on sensor accuracy, Aanderaa should be encouraged to calibrate each Optode individually at the factory – a step they are currently considering.

(3) *Continue analyses of presently collected float data:* With over 70 floats with dissolved oxygen sensors already in the ocean, more detailed analyses of the sensor performance are possible, across a wider range of oceanographic conditions. Researchers should be encouraged to undertake these analyses.

(4) *Improve detailed costs estimates*: This task is directly linked to the determination of the energy budget, since the impact of the oxygen program for the float life time is currently one of the major uncertainties in the cost estimates.

6 Implementation

NOTE: This part of the white paper is currently in development and likely will undergo substantial further changes.

6.1 Overview

At present, there are more than 70 floats deployed in the ocean that have reported oxygen measurements within the last month (see Table A5.1). These floats are located in three clusters: One in the North Pacific, a second one in the South Pacific, and a third one in the North Atlantic (Figure 18). This pattern is not the result of a coordinated effort, but reflects the scientific interests of the pioneering PIs that deployed them. As a result, the currently deployed oxygen equipped floats do not form a larger-scale observing network, although it could provide the seeds for it. Therefore one option for the implementation of the *Argo-Oxygen* program envisioned here is to directly build on these pioneering efforts and simply increase the number of deployments until a satisfactory global network is achieved. However, the current status of the sensor development as well as open issues with regard to communication, data handling, and data quality control suggest that it may be prudent to implement the Argo-Oxygen program in two distinct stages, i.e. a pilot phase, wherein the effort is focused on one or two regions only, followed by the global implementation phase. Detailed planning for both phases is well beyond the scope of this White Paper, so we limit our discussion to the delineation of a road map.

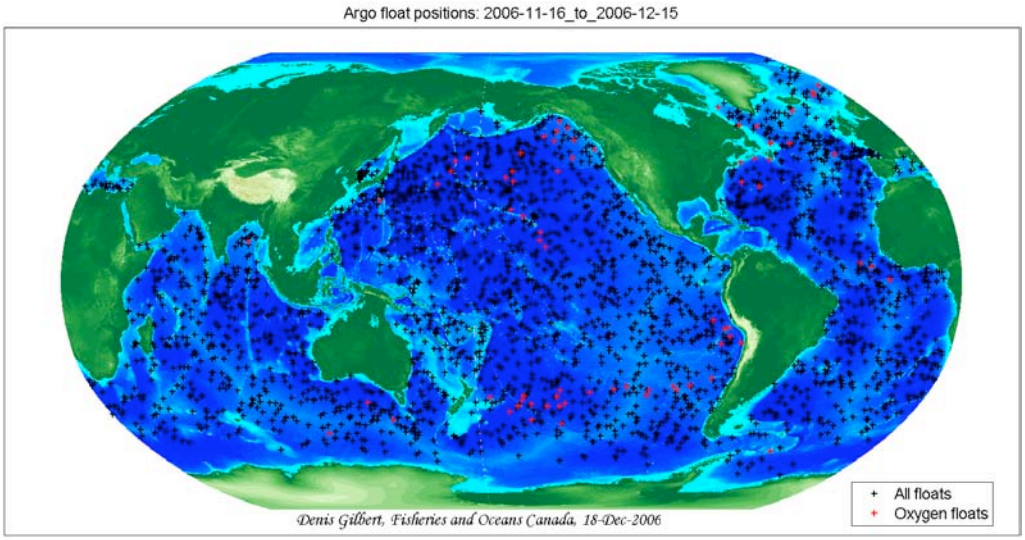

Figure 18. Map showing the locations of the 75 floats that are currently instrumented with dissolved oxygen sensors (current as of 15. December 2006).

6.2 Pilot phase

The main goals of the pilot phase is (i) to prove the feasibility and value of the proposed *Argo-Oxygen* Program, and (ii) to provide for a well-sampled testing ground that permits an examination and solution of outstanding issues associated with sensor quality, data transmission, data handling and data quality control. It will also serve as a pilot project for the development of new data analyses and interpretation approaches, including data

assimilation. Experience from the pilot phase will be directly fed into the planning for the global implementation.

6.2.1 Concept

The concept of the pilot phase is to select one or two regions and instrument them with a large number of floats with oxygen sensors in order to ensure that the spatial and temporal variability of oxygen in this region is well resolved, perhaps even oversampled. It is envisioned that many floats will carry multiple oxygen sensors in order to assess the relative performance of the sensors. The main criterion for determining the selection of the region is that the dynamical nature of its seasonal oxygen cycle is scientifically compelling to warrant such an effort. It will also be advantageous to select a region where regular ship surveys permit the possibility of obtaining bottle samples that can be analyzed by Winkler titration, providing for an absolute reference point. An additional criterion for region selection might include the existence of prior observations, permitting the backward extension of the newly gathered records. Finally, the existence of large range in oxygen concentrations within the water column might be beneficial, as this would allow more thorough tests of the sensor response and stability. Possible candidate regions are the high-latitude North Atlantic (Labrador and Irmiger Seas), the subarctic Pacific, and the regions around the subtropical timeseries stations HOT (Hawaii), BATS (Bermuda), and ESTOC (Canary Islands).

We envision that the pilot phase would last for about two years, in order to ensure thorough testing of the sensors and the observing array, and in order to guarantee the scientific benefit. Planning and initial steps for the global implementation will not have to wait for the end of the pilot phase. In fact, many relevant insights will likely already be available after the first year.

6.2.2 Implementation

In order to avoid interference with the core Argo mission, the pilot phase of the *Argo-Oxygen* program will have to be conducted as an independent project with an independent float deployment plan. We envision that of the order of a few hundred floats with O_2 sensors will be deployed in a relatively tight spatial grid, together with an initial survey of the region's oxygen distribution based on shipboard Winkler titrations. In order to obtain higher frequency data, a fraction of the floats may be programmed to operate on a faster cycle than the typical 10 day repeat cycle of Argo. The region will have to be re-sampled with shipboard-based measurements of oxygen on a regular basis, in order to assess the long-term behavior of the sensors relative to an absolute reference.

This pilot phase may also be used to test other platforms and sensors, such as gliders and a range of other biogeochemical or optical sensors.

6.2.3 Cost

Since the pilot project will be independent from the core Argo activities, the Argo-oxygen program will have to bear the full cost of the floats and the sensors. As a ballpark estimate, the purchase of 100 floats with two oxygen sensors and their operation over 2 years will cost on the order of US$ 2.5 M (see Table 4). Shiptime, salaries, and the cost for making the shipboard Winkler oxygen titration measurements will have to be added to this sum. Although the total cost will depend greatly on the details of the program (number of floats),

the selected region, and the level of ancillary activities, it appears as if a substantial pilot project can be undertaken with a level of funding somewhere between US$ 5M to 10M.

6.2.4 Ancillary Studies

The support of ancillary studies will be of great importance for the success of the pilot project and the demonstration of the feasibility and usefulness of the *Argo-Oxygen* program. These activities will have to include (i) sensor quality assessment studies, (ii) data assemblage and automatic quality control studies, (iii) data interpretation and interpolation studies, (iv) network design and optimization studies, and (iv) studies that attempt to incorporate the observations into modeling frameworks (using diagnostic or inverse methods) in order to take advantage of process information. One example is the incorporation of the oxygen data into biogeochemical models in order to estimate the level of export production.

6.3 Global Implementation

To be written.

7 References

Anderson, L. A., and J. L. Sarmiento (1995), Global ocean phosphate and oxygen simulations, *Global Biogeochem. Cycles*, **9**, 621–636.

Andreev, A., and S. Watanabe Temporal changes in dissolved oxygen of the intermediate water in the subarctic North Pacific, *Geophys. Res. Lett.*, **29**(14), 1680, doi:10.1029/2002GL015021, 2002.

Battle, M., *et al.* (2006), Atmospheric potential oxygen: New observations and their implications for some atmospheric and oceanic models, *Global Biogeochem. Cycles*, **20**, GB1010, doi:10.1029/2005GB002534.

Bender, M., S. Doney, R.A. Feely, I.Y. Fung, N. Gruber, D.E. Harrison, R. Keeling, J.K. Moore, J. L. Sarmiento, E. Sarachik, B. Stephens, T. Takahashi, P.P. Tans, and R. Wanninkhof, A Large-Scale Carbon Observing Plan: In Situ Oceans and Atmosphere (LSCOP), pp. 201, Nat. Tech. Info. Services, Springfield, 2002.

Benitez-Nelson, C., K. O. Buesseler, D. M. Karl and J. Andrews (2001) A time-series study of particulate matter export in the North Pacific subtropical gyre based on ^{234}Th: ^{238}U disequilibrium, Deep-Sea Res. I, 48, 2595-2611.

Bindoff, N. L., and T. J. McDougall (2000), Decadal changes along an Indian Ocean section at 32 degrees S and their interpretation, *J. Phys. Oceanogr.,* **30**, 1207– 1222.

Bopp, L., C. LeQuéré, M. Heimann, A. C. Manning, and P. Monfray (2002) Climate-induced oceanic oxygen fluxes: Implications for the contemporary carbon budget, *Global Biogeochem. Cycles*, **16**, 1022, doi:10.1029/2001GB001445.

Carlson, C.A., Ducklow, H.W. & Michaels, A.F. (1994) Annual flux of dissolved organic carbon from the euphotic zone in the northwestern Sargasso Sea. *Nature* **371**, 405, 40

Clark LC, Wolf R, Granger D, Taylor Z (1953). Continuous recording of blood oxygen tensions by polarography. J Appl Physiol. 6, 189-193.

Deutsch, C., S. R. Emerson, and L. Thompson (2005). Fingerprints of climate change in North Pacific oxygen, *Geophys. Res. Lett.*, **32**, L16604, doi:10.1029/2005GL023190.

Deutsch, C., S. Emerson, and L. Thompson (2006), Physical-biological interactions in North Pacific oxygen variability, *J. Geophys. Res.,* **111**, C09S90, doi:10.1029/2005JC003179.

Dittmar, W. (1884). Report on researches into the composition of ocean water collected by H.M.S. Challenger during the years 1873-1876. In: (J. Murray, ed) Report on the Scientific Results of the Voyage of H.M.S. Challenger: Physics and Chemistry, Vol. 1, part 1, London, H.M. Stationery Office, 251 pp.

Doney, S.C., J.L. Bullister, and R. Wanninkhof, 1998: Climatic variability in upper ocean ventilation diagnosed using chlorofluorocarbons, *Geophys. Res. Lett.*, **25**, 1399-1402.

Emerson, S., P. D. Quay, C. Stump, D. Wilbur & M. Knox (1991) O_2, Ar, N_2 and ^{222}Rn in surface waters of the subarctic ocean: Net biological O2 production, *Global Biogeochem. Cycles*, 5, 4969.

Emerson, S., P. Quay, D. Karl, C. Winn, L. Tupas, and M. Landry (1997) The carbon pump in the Subtropical Pacific Ocean: Implications for the Global Carbon Cycle, *Nature* , 389, 951- 954.

Emerson, S., Y.W. Watanabe, T. Ono, and S. Mecking (2004). Temporal trends in apparent oxygen utilization in the upper pycnocline of the North Pacific: 1980-2000. *J. Oceanogr.* **60**: 139-147.

Freeland, H.J. and P.F.Cummins (2005) Argo: A new tool for environmental monitoring and assessment of the world's ocean, an example from the NE Pacific. *Progress in Oceanography*, **64**(1), 31-44.

Ganachaud, A., and C. Wunsch (2002), Oceanic nutrient and oxygen transports and bounds on export production during the World Ocean Circulation Experiment, *Global Biogeochem. Cycles*, **16**(4), 1057, doi:10.1029/2000GB001333.

Garcia, H., A. Cruzado, L. Gordon, and J. Escanez (1998), Decadal-scale chemical variability in the subtropical North Atlantic deduced from nutrient and oxygen data, *J. Geophys. Res.*, **103**, 2817– 2830.

Garcia, H. E., and Keeling (2001) On the global seasonal air-sea oxygen flux. *Journal of Geophysical Research,* **106**, 31155-31166.

Gilbert, D., B. Sundby, C. Gobeil, A. Mucci and G.-H. Tremblay (2005) A seventy-two year record of diminishing deep-water oxygen in the St. Lawrence estuary: The northwest Atlantic connection, *Limnol. Oceanogr.,* **50** (5): 1654-1666

Gould, J., and the Argo Science Team, 2004. Argo Profiling Floats Bring New Era of In Situ Ocean Observations. *EoS, Transactions of the American Geophysical Union*, **85**(19), 11 May 2004.

Gould, W.J. and J. Turton (2006) Argo – Sounding the Oceans. *Weather*, **61**(1), 17-21.

Gouretski, V., and K. P. Koltermann (2007), How much is the ocean really warming?, *Geophys. Res. Lett.,* **34**, L01610, doi:10.1029/2006GL027834.

Grantham, B.A., F. Chan, K.J. Nielsen, D.S. Fox, J.A. Barth, A. Huyer, J. Lubchenco and B.A. Menge (2004) Upwelling-driven nearshore hypoxia signals ecosystem and oceanographic changes in the northeast Pacific. *Nature*, **429**: 749-754.

Gruber, N., J. L. Sarmiento, and T. F. Stocker (1996) An improved method for detecting anthropogenic CO_2 in the oceans, *Global Biogeochem. Cycles,* **10**, 809–837.

Gruber, N., C. D. Keeling and T. F. Stocker 1998) Carbon-13 constraints on the seasonal inorganic carbon budget at the BATS site in the northwestern Sargasso Sea. *Deep-Sea Res. I*, 45, 673-717.

Gruber, N., E. Gloor, S.-M. Fan, and J. L. Sarmiento (2001), Air-sea fluxes of oxygen estimated from bulk data: Implications for the marine and atmospheric oxygen cycles, *Global Biogeochem. Cycles*, 15, 783–804.

Hamme, R. C. and S. R. Emerson (2006) Constraining bubble dynamics and mixing with dissolved gases: Implications for productivity measurements by oxygen mass balance, Jour. Mar. Res., 64, 73-95.

Helland-Hansen, B. and F. Nansen (1909). The Norwegian Sea: its physical oceanography based upon the Norwegian researches 1900-1904. Report on Norwegian Fishery and Marine Investigations, 2(2), Kristiania, 390 pp.

Henry-Edwards, H., M. Tomczak (2006) Detecting changes in Labrador Sea Water through a water mass analysis of BATS data. *Ocean Science,* **2:** 19-25.

Holfort, J., K. M. Johnson, B. Siedler, and D. W. R. Wallace (1998), Meridional transport of dissolved inorganic carbon in the South Atlantic Ocean, *Global Biogeochem. Cycles*, **12**(3), 479– 499.

IMBER/SOLAS (2006). Joint SOLAS-IMBER Ocean Carbon Research: Implementation Plan, http://www.imber.info/products/Carbon_Plan_final.pdf.

Jenkins, W. and S. Doney (2003) The subtropical nutrient spiral, *Glob. Biogoechem. Cycles*, 17, doi: [10.1029/2003GB002085]

Jenkins, W. J. and D. W. R. Wallace (1992) Tracer based inferences of new primary production in the sea, pp. 299-316, In: Primary Production and Biogeochemical Cycles in the Sea, (ed., P. G. Falkowski and A. D. Woodhead) Plenum N. Y.

Jin, X, R. G. Najjar F. Louanchi and S. C. Doney (2007) A modeling study of the seasonal oxygen budget of the global ocean, *J. Geophys. Res.* (in press).

Johnson, G. C. and N. Gruber (2007). Decadal water mass variations along 20°W in the northeastern Atlantic Ocean. *Prog. Oceanogr.*, in press.

Johnson, K. S., J. A. Needoba, S. C. Riser, and W. J. Showers (2007) Chemical sensor networks for the aquatic environment. Chemical Reviews, in press.

Joos, F., G.-K. Plattner, T.F. Stocker, A. Körtzinger, and D.W.R. Wallace (2003). Trends in marine dissolved oxygen: Implications for ocean circulation changes and the carbon budget. *EOS Trans. AGU* **84**: 197-204.

Karstensen, J., M. Tomczak (1998) Age determination of mixed water masses using CFC and oxygen data. *J. Geophys. Res.,* **103(C9):** 18599-18609.

Kasai, A., T. Yamada, and H. Takeda (2007) Flow structure and hypoxia in Hiuchi-nada, Seto Inland Sea, Japan, *Estuarine Coastal and Shelf Science*, **71** (1-2): 210-217.

Keeling, R.F., and H. Garcia (2002). The change in oceanic O_2 inventory associated with recent global warming. *Proc. US Natl. Acad. Sci.* **99**, 7848-7853.

Keeling, R. F., and S. R. Shertz, Seasonal and interannual variations in atmospheric oxygen and implications for the global carbon cycle, *Nature*, **358**, 723– 727, 1992.

Keeling, R. F., S. C. Piper, and M. Heimann, Global and hemispheric CO_2 sinks deduced from changes in atmospheric O_2 concentrations, *Nature*, **381**, 218– 221, 1996.

Keeling, R. F., and T.-H. Peng, Transport of heat, CO_2 and O_2 by the Atlantic's thermohaline circulation, *Philos. Trans. R. Soc. London, Ser. B*, **348**, 133– 142, 1995.

Keeling, R.F., B. B. Stephens, R. G. Najjar, S. C. Doney, D. Archer, and M. Heimann (1998) Seasonal variations in the atmospheric O_2/N_2 ratio in relation to the kinetics of air-sea gas exchange. *Global Biogeochemical Cycles*, **12**, 141-163.

Keeling, C. D., H. Brix, and N. Gruber (2004), Seasonal and long-term dynamics of the upper ocean carbon cycle at Station ALOHA near Hawaii, *Global Biogeochem. Cycles*, **18**, GB4006, doi:10.1029/2004GB002227.

Keller, K., R. D. Slater, M. Bender, and R. M. Key (2002), Possible biological or physical explanations for decadal scale trends in North Pacific nutrient concentrations and oxygen utilization, *Deep Sea Res., Part II*, **49**, 345–362.

Körtzinger, A., J. Schimanski, and U. Send (2005). High-quality oxygen measurements from profiling floats: A promising new technique, *J. Atm. Ocean. Techn.* **22**, 302-308.

Körtzinger, A., J. Schimanski, U. Send, and D.W.R. Wallace (2004). The ocean takes a deep breath. *Science* **306**: 1337.

Körtzinger, A., S. C. Riser, and N. Gruber (2006) Oceanic oxygen: the oceanographer's canary bird of climate change. *ARGO Newsletter*, **7**, June 2006, 2-3.

Laws, E., P. Falkowski, W. O. Smith, H. Ducklow, and J. J. McCarthy (2000) Temperature effects on export production in the open ocean. *Global Biogeochem. Cycles*, **14**, 1231-1246.

Levitus, S., J. Antonov, and T. Boyer (2005), Warming of the world ocean, 1955–2003, *Geophys. Res. Lett.,* **32**, L02604, doi:10.1029/2004GL021592.

Levitus, S., J. Antonov, T. P. Boyer, and C. Stephens (2000), Warming of the world ocean, *Science*, **287**, 2225– 2229.

LeQuéré, C., *et al.* (2003), Two decades of ocean CO_2 sink and variability, *Tellus*, **55B**, 649–656.

Manning, A. C., and R. F. Keeling (2006), Global oceanic and land biotic carbon sinks from the Scripps atmospheric oxygen flask sampling network, *Tellus, Ser. B.,* **58**, 95–116.

Matear, R. J., A. C. Hirst, and B. I. McNeil (2000), Changes in dissolved oxygen in the Southern Ocean with climate change, *Geochem. Geophys. Geosyst.,* **1**(11), doi:10.1029/2000GC000086.

Matear, R. J., and A. C. Hirst, Long-term changes in dissolved oxygen concentrations in the ocean caused by protracted global warming, *Global Biogeochem. Cycles*, **17**(4), 1125, doi:10.1029/2002GB001997, 2003.

McDonagh, E. L., H. L. Bryden, B. A. King, R. J. Sanders, S.A. Cunningham and R. Marsh. 2005. Decadal changes in the South Indian Ocean thermocline, *Journal of Climate*, **18**, 1575-1590.

Mosedale, T.J., D.B. Stephenson, M. Collins, T.C. Mills (2006). Granger Causality of Coupled Climate Processes: Ocean Feedback on the North Atlantic Oscillation. *J. Climate,* **19:** 1182-1194.

Najjar, R G. and R. F. Keeling (1997) Analysis of the mean annual cycle of the dissolved oxygen anomaly in the World Ocean. *J. Mar. Res.* 55, 117-151.

Najjar, R., and R. Keeling, The mean annual cycle of the air-sea oxygen flux: A global view, *Global Biogeochem. Cycles*, **14**(2), 573– 584, 2000.

Najjar, R.G., X. Jin, F. Louanchi, O. Aumont, K. Caldeira, S.C. Doney, J.-C. Dutay, M. Follows, N. Gruber, F. Joos, K. Lindsay, E. Maier-Reimer, R.J. Matear, K. Matsumoto, P. Monfray, A. Mouchet, J.C. Orr, G.K. Plattner, J.L. Sarmiento, R. Schlitzer, M.F. Weirig, Y. Yamanaka and A. Yool, Impact of circulation on export production, dissolved organic matter and dissolved oxygen in the ocean: Results from OCMIP-2, *Global Biogeochem. Cycles, submitted.*

Ono, T., T. Midorikawa, Y. W. Watanabe, K. Tadokoro, and T. Saino (2001), Temporal increases of phosphate and apparent oxygen utilization in the subsurface waters of western subarctic Pacific from 1968 to 1998, *Geophys. Res. Lett.,* **28**, 3285– 3288.

Plattner, G.-K., F. Joos, and T. F. Stocker, Revision of the global carbon budget due to changing air-sea oxygen fluxes, *Global Biogeochem. Cycles*, **16**(4), 1096, doi:10.1029/2001GB001746, 2002.

Quay, P. and J. Stutzman (2003) Surface layer carbon budget for the subtropical N. Pacific: _^{13}C constraints at station ALOHA, *Deep-Sea Res. I*, **50**, 1045-1061.

Rabalais, N.N. and R.E. Turner (2001) Commonality and the future. In *Coastal Hypoxia Consequences for living resources and Ecosystems*, Eds: N.N Rabalais and R.E. Turner, American Geophysical Union, Coastal and Estuarine Studies, **58**: 451-454.

Redfield, A. C., B. H. Ketchum and F. A. Richards (1963) The influence of organisms on the composition of seawater, In: *The Sea*, Vol 2, M.N. Hill editor, Interscience, New York, pp. 26-77.

Schlitzer, R. (2000) Applying the adjoint method for biogeochemical modeling: Export of particulate organic matter in the world ocean, In: *Inverse Methods in Global Biogeochemical Cycles*, Geophysical Monograph 114, Amer. Geophys. U. , Washington, D.C.

Service, R. (2004) New dead zone off Oregon Coast hints at sea change in currents. *Science*, **305**, 1099.

1099.Shaffer, G., O. Leth, O. Ulloa, J. Bendtsen, G. Daneri, V. Dellarossa, S. Hormazabal, and P. I. Sehlstedt (2000), Warming and circulation change in the eastern South Pacific Ocean, *Geophys. Res. Lett.*, **27**, 1247– 1250.

Spitzer, W.S. and W.J. Jenkins (1989), Rates of vertical mixing, gas exchange and new production: Estimates from seasonal gas cycles in the upper ocean near Bermuda. *J. Mar. Res.,* 47, 169-196.

Stephens, B. B., R. F. Keeling, M. Heimann, K. D. Six, R. Murnane, and K. Caldeira (1998), Testing global ocean carbon cycle models using measurements of atmospheric O_2 and CO_2 concentration, *Global Biogeochem. Cycles*, **12**(2), 213– 230.

Tengberg, A.; Hovdenes, J.; Andersson, H. J.; Brocandel, O.; Diaz, R.; Hebert, D.; Arnerich, T.; Huber, C.; Kortzinger, A.; Khripounoff, A.; Rey, F.; Ronning, C.; Schimanski, J.;

Sommer, S.; Stangelmayer (2006) A. Evaluation of a lifetime-based optode to measure oxygen in aquatic systems, *Limnol. Oceanogr. Methods*, **4**, 7-17.

Tomczak, M. 1999. Some historical, theoretical and applied aspects of quantitative water mass analysis. *J. Mar. Res.,* **57:** 275-303.

Wallace, D.W.R. (1995), *Monitoring global ocean inventories*, OOSDP Background Rep. 5, 54 pp., Ocean Observ. Syst. Dev. Panel, Texas A&M Univ., College Station, TX.

Watanabe, Y. W., T. Ono, A. Shimamoto, T. Sugimoto, M. Wakita, and S. Watanabe (2001), Probability of a reduction in the formation rate of the subsurface water in the North Pacific during the 1980s and 1990s, *Geophys. Res. Lett.,* **28**, 3289– 3292.

Winkler, L.W. (1888). Die Bestimmung des im Wasser gelösten Sauerstoffes. *Ber. Dtsch. Chem. Ges.* **21**: 2843-2855.

Wust, G. Schichtung und Zirkulation des Atlantischen Ozeans, Wiss. Ergebn. Deutsch. Atlant. Exped Forsch. Schiff "Meteor" 1925_27 6 (1936); (Engl. transl.) The Stratosphere of the Atlantic Ocean (ed. Emery, W.) (Amerind, New Delhi, 1978).

8 Appendix:

8.1 Laboratory assessment of dissolved oxygen sensors (Steve Riser)

In order to investigate the behavior of the Optode sensor in a more quantitative way, a laboratory experiment was set up at the University of Washington to examine the characteristics of several Optodes as functions of pressure and temperature in a controlled environment. Five Optodes were placed in a sealed container that was filled with deionized water having a known O_2 concentration. Cables supplying power to the Optodes and carrying output data were run through the container. The entire apparatus was then placed in a temperature-controlled chamber. The water in the container was stirred. The temperature was then slewed through various values from 1–30 °C, and the values of dissolved O_2 as measured by the Optodes were recorded. There was often a strong temperature sensitivity to the Optode behavior, even when the factory-supplied calibrations were taken into effect (Fig. A.11).

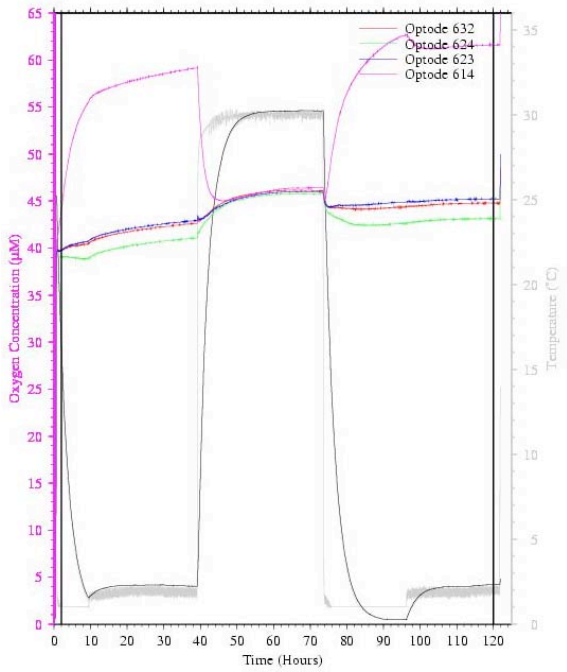

Figure A1.1: Results from a laboratory experiment carried out at the University of Washington showing the behavior of 5 Optodes in a closed, water-filled container, at a fixed concentration of dissolved O_2. The water in the container was stirred. The container was placed in a temperature-controlled chamber, and the temperature was slewed between 2 °C and 30 °C over the course of 5 days (the light grey line). The measured values of O_2 at the 5 sensors, shown by the colored lines, indicate that some have a large temperature coefficient that is unaccounted for in the factory calibration. The experiment was carried out at a constant pressure of 1 atmosphere.

The temperature in the chamber began at 20 °C and was lowered to 2 °C as the experiment was started (Fig. A1.1). After about 10 hours, the water in the closed container had equilibrated to the new temperature, and as can be seen, two of the Optodes (614 and 625) showed large changes with temperature; Optode 623 decreased in concentration by nearly 35 µmol kg^{-1} from its initial value, while Optode 614 increased by nearly 20 µmol kg^{-1}. The other instruments changed by < 5 µmol kg^{-1}. As the temperature was increased to 25 °C, the

three most stable sensors increased by ~ 5 μmol kg^{-1}, while Optode 614 increased by nearly 50 μmol kg^{-1} and Optode 625 decreased by about 15 μmol kg^{-1}. When the temperature returned to 2 °C, the behavior of sensors 614 and 623 reversed again, but the measured values did not return to the values they measured initially at 2 °C. This suggests that there is some variation in the performance of Optodes from sensor-to-sensor, and that even after the sensors have left the factory careful calibration is required. At the present time, Aanderaa only calibrates about 4% of the sensors in each batch and applies the measured calibration coefficients from these instruments to the entire batch. These results suggest that this procedure is not sufficient, as 2 out of the 5 sensors examined here (40%) behaved far differently from the median of the ensemble. This apparent temperature dependence to the sensor output could conceivably account for some of the instrument-to-instrument variations measured in the ocean (Fig. 16). An analogous set of experiments carried out with IDO sensors showed little, if any, temperature dependence to the sensor output once the factory-supplied calibration coefficients were applied.

The experiment described above was carried out at a constant pressure of 1 atmosphere. In addition to this experiment, there was an attempt to investigate pressure-dependent effects by the UW group (Fig. A1.2). In this case, both IDO and Optode-equipped APEX floats were placed into a large, water-filled pressure vessel that is routinely used at UW for ballasting all floats prior to deployment. The temperature in the vessel was fairly constant at about 18 °C. The Optode floats measured the dissolved O_2 in the water as a function of pressure in the tank (the floats were running during the experiment, with the output from the sensors brought out of the tank with sealed cables), as the pressure was increased from 0 to 1000 decibars. The 3 Optode floats examined in this manner showed almost no pressure dependence to their measured O_2 values over the entire pressure range, which would be expected if the manufacturer's calibration is correct (there is a weak pressure dependence included in the Optode calibration).

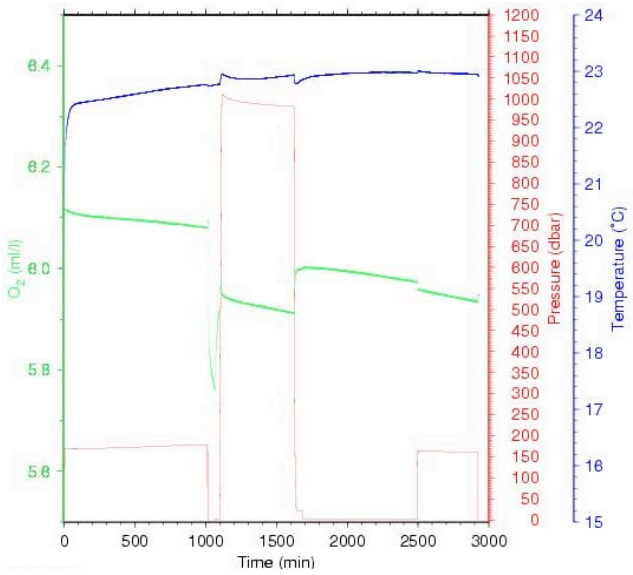

Figure A1.2: Measured O_2 as a function of pressure and time for IDO number 2216. Note the decrease in measured O_2 (the green line) when the pressure is increased from 0 to 1000 decibars (red line). In this case the temperature also increased slightly due to the compression of the water in the vessel (an adiabatic effect). For a 1000 decibar change in pressure the dissolved O_2 changes by about 0.2 ml/l, or about 8 μmol kg^{-1} in this case, a sizable amount. The slow change in O_2 over the course of the experiment is due to a slight leakage of water through the Tygon tubing used to seal the CTD cell.

On the other hand, the 3 IDO floats examined in this experiment did show noticeable pressure effects on their measured O_2. Since there were impurities (oil) known to be present in the water in the pressure vessel, the CTDs on the IDO floats were protected by filling the $CTDO_2$ cell with dionized water, connecting the input port of each cell to the exhaust port, and then turning on the CTD pump. The result was that each IDO was repeatedly sampling the same dionized water, and it should be expected that the measured O_2 concentrations should be nearly constant (except for perhaps a small, steady amount of O_2 consumption). The pressure was then cycled between 0 and 1000 decibars. As can be seen in Fig. 7, there was an apparent pressure-related change in the measured O_2 concentration of as much as 8 μmol kg^{-1} on one of the IDO instruments tested, with the measured values too small at high pressures (smaller but similar results were found on the other two). Thus, there appears to be a possible pressure effect with IDO sensors that is not accounted for by the manufacturer's calibrations.

There is evidence from the field that such pressure-related errors do indeed occur with IDO sensors. Float WMO 4900093, which operated near the HOT site for over 3 years, appears to show just such an effect (Fig. A1.3).

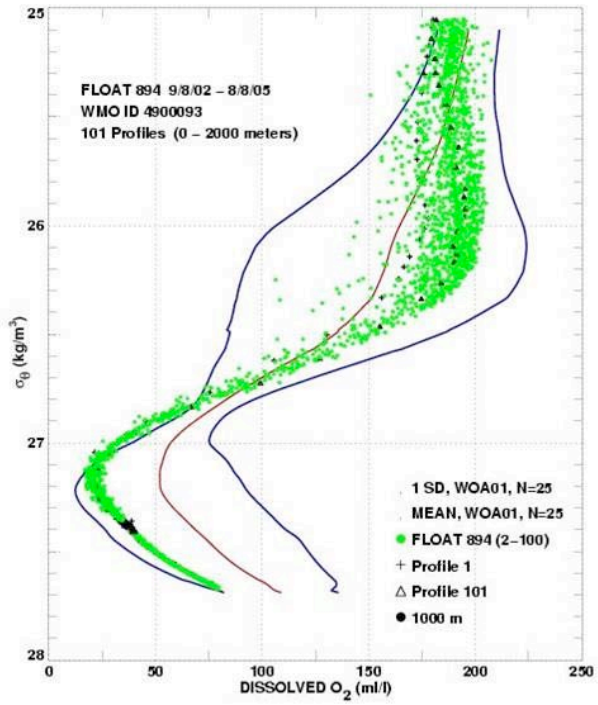

Figure A1.3: Dissolved O_2 from float WMO 4900093 (UW), located near Hawaii, plotted against potential density (green dots). Also shown are the mean of the historical data from this region (red line) and the one standard deviation envelope of the historical data (blue lines). Note that at potential densities less than about 26.8 the float-measured O_2 values and this historical mean do not differ substantially, but at potential densites greater than 26.8 the float-derived values are consistently less than the historical mean, in some cases lying outside of the one standard deviation line. Since the historical data points were all measured using Winkler methods, it can be inferred that the IDO measurements are in error.

The systematic difference between the IDO measurement and historical data at high pressures appears to be consistent with the UW laboratory measurements. At a pressure of 1000 decibars (the black dots in Fig. A1.3) the IDO is 8-10 μmol kg^{-1} lower than the historical mean value for the region, similar to the differences measured in the pressure vessel (Fig.

A1.2). These differences have been noted by SeaBird, and steps to correct this pressure dependence have been taken in IDO units manufactured since mid-2005. The unwanted pressure dependence appeared to be caused by at least two effects. First, a pressure dependent term is included in the calibration equation for each IDO, but the calibration coefficient for pressure was not measured uniquely for each manufactured sensor. Instead, the value was measured once when production began in 2002 and the same value was used for each sensor until mid-2005. To remedy this, SeaBird now measures the pressure effect of each IDO sensor in fresh water at a given temperature at the factory and applies this unique coefficient to each unit, with the hoped-for effect of reducing the pressure dependence shown in Figures A1.2 and A1.3. A second remedy is perhaps more significant: it has been noted at SeaBird that the diffusion of O_2 through the membrane on IDO sensors is a function of temperature and pressure, hence the variable sensor response time given in Table 1. Until mid-2005, this variable diffusion time was not taken into account in the operation of the IDO sensor. Roughly speaking, at high pressures and lower temperatures the diffusion through the membrane is slower, so that over a given time less O_2 will have diffused through the membrane to be reduced at the cathode, yielding lower apparent values of O_2 at higher pressures. To remedy this, the pumping algorithm of the SeaBird CTD unit was changed so that the pumping time for a single sample is increased at higher pressures, allowing enough time for the O_2 to fully diffuse across the membrane so that the pressure dependence is removed. Results from IDO sensors deployed since mid-2005 have been greatly improved due to these efforts.

8.2 Field experience: The Canadian Program (from Denis Gilbert)

As part of the Canadian Argo program, the Department of Fisheries and Oceans (DFO) deployed 15 Webb Research Corporation APEX profiling floats equipped with Aanderaa Optode sensors in 2004 and 2005: two in the northwest Atlantic Slope Water (4900497 and 4900627), one in the Labrador Sea (4900494), and two in the northeast Pacific (4900523 and 4900637). In Fig. A2.1a, we have indicated the launch positions of the floats with triangles, and their most recent positions in June 2006 with squares. Floats 4900494 and 4900497 travelled 530 km and 1150 km respectively, but the other three floats are still within 200 km of their initial positions. The latest oxygen profiles from June 2006 for each float are shown in Fig. A2.1b. Here we report on the first two years of oxygen data from these floats, and we briefly discuss the scientific motivations behind this *Argo-Oxygen* pilot study.

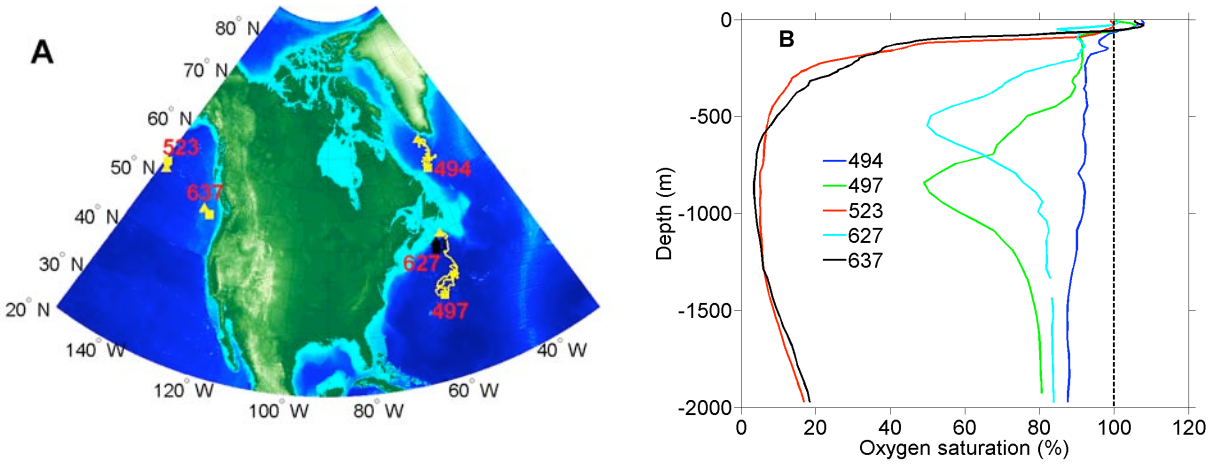

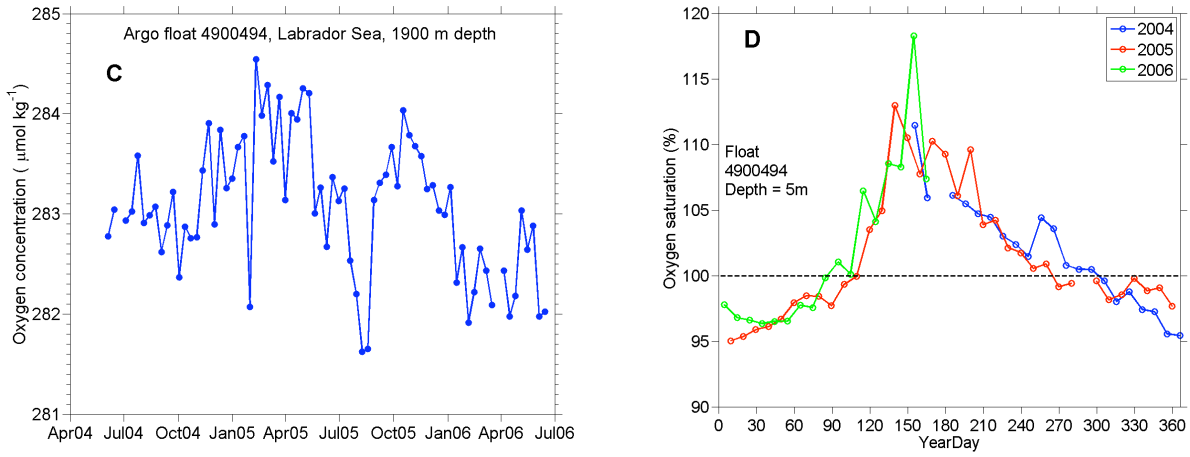

Figure A2.1. a) Map showing the locations of the five DFO *Argo-Oxygen* floats deployed during 2004 and 2005. b) Vertical profiles of oxygen saturation measured between June 8 and June 14, 2006. Float 4900494 time series of b) oxygen concentration at 1900 m depth, and d) oxygen saturation at 5 m depth.

A rare opportunity to compare Argo-Optode oxygen measurements with Winkler titrations occurred in early September 2004 for float 4900523. The results were very encouraging, with an average absolute difference as small as 6.2 μmol kg^{-1}. This is within the manufacturer's specified accuracy of 8 μmol kg^{-1}. In absence of nearby Winkler titrations to check for sensor drift over time, an alternative is to look for oxygen trends at great depths, where we expect fairly stable values in oceanic regions with weak horizontal gradients of T-S-O_2 properties. Fig. A2.1c shows that for float 4900494, in the Labrador Sea, there is no evidence of oxygen sensor drift (to within ± 1 μmol kg^{-1}) at 1900 m depth over the first two years. In the surface layer, where physical and biological processes may cause departures from gas equilibrium with the atmosphere (100% oxygen saturation), we see a seemingly repeatable annual cycle of undersaturation from December to March and supersaturation from April to October (Fig. A2.1d).

There are many factors that make oxygen an interesting parameter to measure in the ocean. Float 4900494 is in a region of active deepwater formation, where homogeneous, elevated oxygen values over several hundreds of meters can provide useful evidence of recent surface ventilation. We deployed floats 4900497 and 4900627 near the Laurentian Channel mouth, where changing oxygen concentrations can either improve or worsen the hypoxic conditions that have prevailed in the bottom waters of the Lower St. Lawrence Estuary since the mid-1980s. Finally, floats 4900523 and 4900637 are monitoring the northeast Pacific oxygen minimum zone (OMZ).

Time-depth contours of temperature, salinity, density and oxygen from float 4900637 are shown in Fig. A2.2. There is a 500 m thick layer of oxygen saturations below 5% centred at about 1000 m depth. Interestingly, in early May 2006, this float entered a region with very different T-S-O_2 properties as it moved east of the 129°W meridian, near 47°N. The 30% oxygen saturation level then underwent a spectacular 240 m upward excursion. We believe the low oxygen waters encountered since May 2006 by float 4900637 are of continental slope origin. These waters, often considered to be the California Undercurrent with a warm and salty nature, can have oxygen lower than offshore waters by as much as 100 _mol kg^{-1} on the 26.5 or 26.7 isopycnal surface.

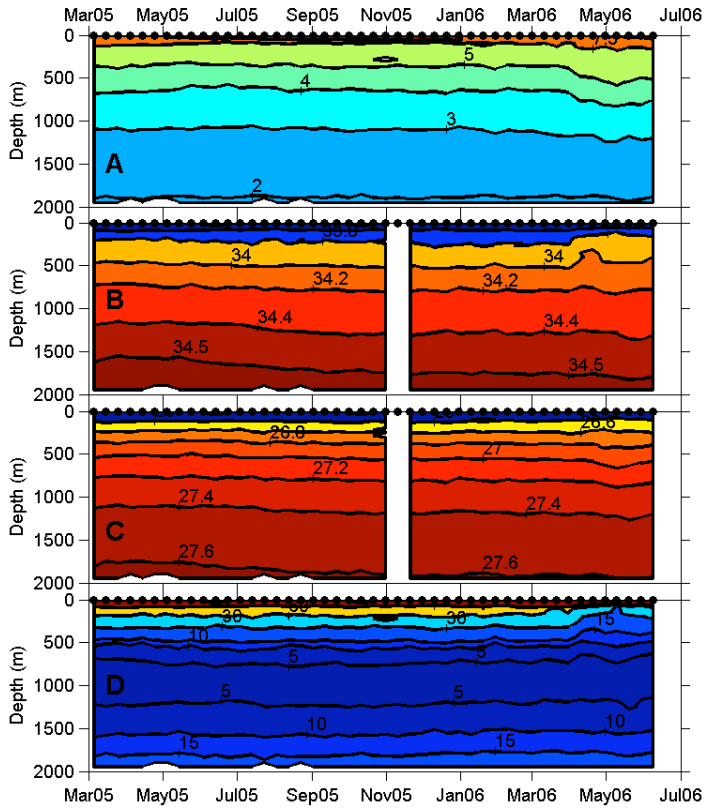

Figure A2.2:. Float 4900637 measurements of A) temperature (°C), B) salinity, C) potential density (kg m^{-3}), and D) oxygen saturation (%). The black dots at the top indicate the times of sampling.

8.3 Field experience: Japan Argo Program (from Taiyo Kobayashi)

Since Feb. 2005, JAMSTEC has operated floats with both IDO (SBE43) and Optode oxygen sensors as a part of the Japanese Argo Program. Through the end of Dec. 2006, 9 oxygen sensor equipped floats have been deployed (6 for the Japan Agency for Marine-Earth Science and Technology (JAMSTEC) and 3 for Tohoku University) in the North Pacific (see Table A3.1 and Figure A3.1). All of them have continued their operation successfully except for WMO2900460, which had a gap for a series of 7 profiles due to insufficient buoyancy.

Compared with the shipboard bottle sampling observations at the deployments, our first profiles show systematic negative biases that are greater than the nominal measurement errors of the oxygen sensors and occur irrespective of the sensor type, i.e. Optode or IDO (SBE43). In the deeper layer, typical offsets are about 0-10 μ-mol kg-1. The offsets are larger in the upper layers, with the maximum differences exceeding 40 μ-mol kg-1. Although it must be considered that both measurements are 10 days and up to 100 km apart in a region with strong fronts, these large (and systematic) differences are hardly caused by variability of the ocean (e.g., meso-scale eddies), but largely reflect sensor biases.Table A3.1: Summary of the Argo floats with oxygen sensors deployed by Japanese groups.

WMO ID	Deployment date and location		Sensor	Depth [dbar]		Levels	Cycle	No. Prof.	Ship
	Date	Location		Parking	Profile		[day]		
Tohoku Univ.									
2900460 †	2005/2/23	41.006° N 167.410° E	Optode	26.35_ _	2000	59	7	89#	R/V Shoyo-maru
2900616 ‡	2006/2/25	32.350° N 144.587° E	SBE 43	1000	1000	91	5	62	R/V Hakuho-maru
4900905 †	2006/7/8	36.511° N 164.972° W	Optode	26.1_ _	1500	96	7	25	R/V Oshoro-maru
JAMSTEC									
2900514	2005/6/24	41.012° N 164.975° E	Optode	1000	2000	115	10	55	R/V Ryofu-maru
2900540	2005/6/24	40.013° N 165.032° E	SBE 43	1000	2000	115	10	55	R/V Ryofu-maru
2900541	2005/6/24	39.020° N 164.983° E	Optode	1000	2000	115	10	55	R/V Ryofu-maru
2900542	2005/6/25	38.002° N 165.007° E	Optode	1000	2000	115	10	55	R/V Ryofu-maru
4900651	2005/7/31	39.014° N 164.989° W	Optode	1000	2000	115	10	51	R/V Oshoro-maru
4900652	2005/8/1	36.998° N 164.941° W	SBE 43	1000	2000	115	10	51	R/V Oshoro-maru

NOTES: †: Drifting on the isopycnal surface of 26.35_ and 26.1_, respectively. ‡: Chlorophyll and nephelometric turbidity sensors are also equipped. The number of profiles represents the profiles measured by the corresponding float (#: The cycle number is 96 due to not surfacing during the cycle 84-90, as of the end of Dec. 2006).

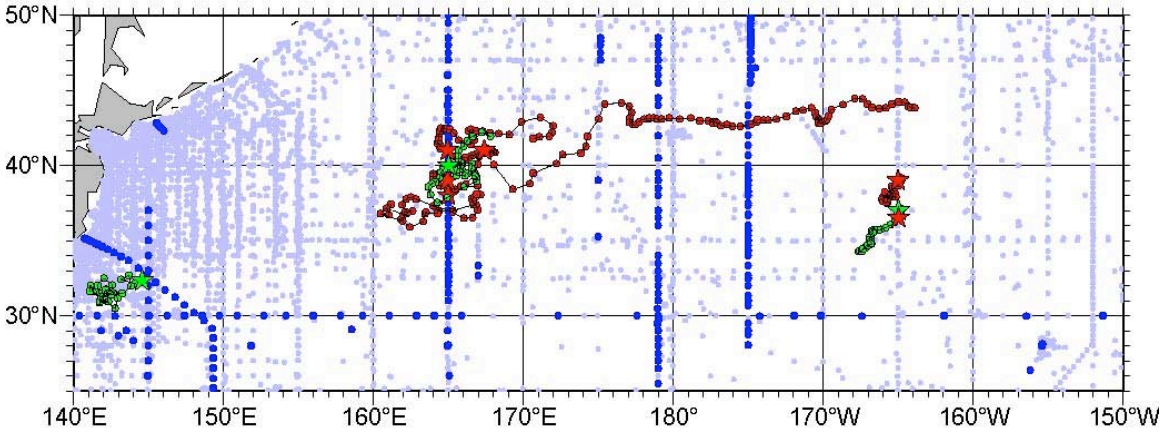

Figure A3.1: Locations of float deployments (stars) and their measurements (circles, as of July 12, 2006). The colors indicate the type of oxygen sensors employed: red: Optode, and green: IDO (SBE43). The light-blue and blue dots represent historical oxygen observations by bottle sampling and CTD in World Ocean Database 2001 (WOD01).

Larger negative biases are found in regions where the vertical gradient of oxygen is large. This suggests that one of the major causes of these negative biases may be the slow response of the oxygen sensor, and that the equilibration time of the sensors might be longer than advertised (see Table 2 in text). However, this does not explain the negative bias below 1000 dbar (below 3°C) as concentration and temperature gradients are very small.

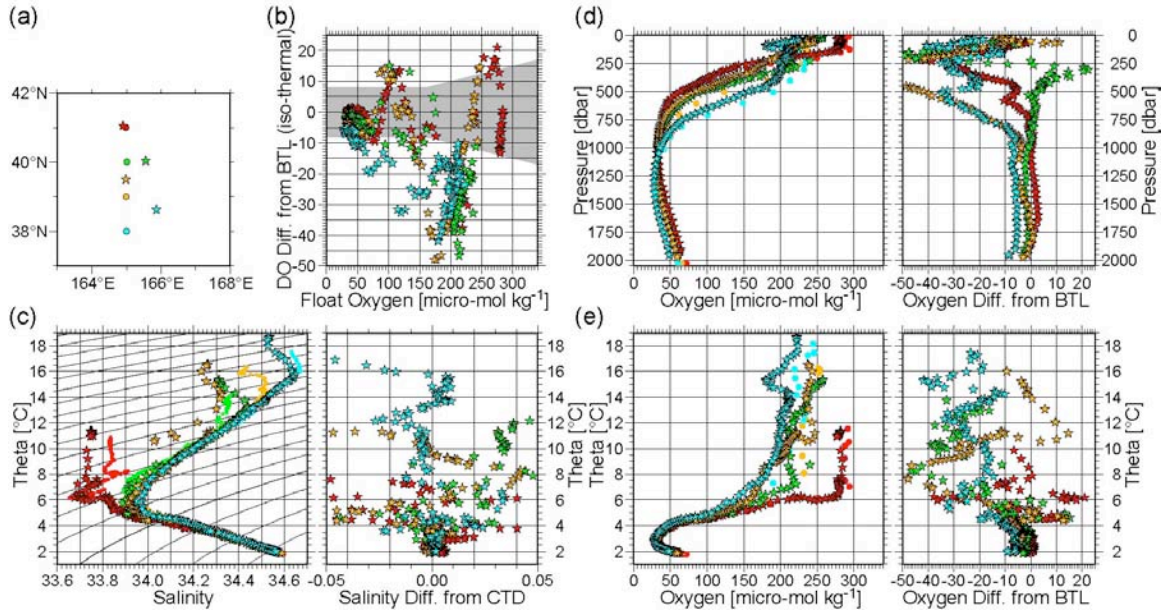

Figure A3.2: Comparison of measurements from the first float profiles (stars) and shipboard observations (circles) right after the deployment of the floats. The first float profiles were usually taken about 10 days after deployment. All floats are equipped with an Optode sensor except for one that carries on IDO (SBE43).

(a) Horizontal locations of the float and shipboard measurements. (b) Oxygen difference on the isothermal layer (float-shipboard: unit is micro-mol kg^{-1}) as a function of the float measured oxygen. The shaded region represents the error expected from the Optode sensor (c) Theta-salinity plot of the profiles, and the difference of the float salinity measurement versus the float measured theta (on isotherms). (d) Vertical profiles of oxygen and difference of the float oxygen from the bottle oxygen (on isobars). (e) Oxygen versus theta and oxygen difference between float and bottle versus theta (on isotherms).

As explained in the main text, the temperature sensor of the Optode has a long equilibration time, potentially explaining some of the biases. Figure A3.3 shows the temperature difference measured by CTD and Optode sensors for WMO ID 2900542 (the cyan float in Figure A3.2). The Optode thermistor has a substantial negative temperature bias of about 0.03 to 0.05°C in the deepest layers, and the bias increases to more than 0.2°C in the thermocline and exceeds 0.4°C near the surface. This bias is almost proportional to the vertical gradient of temperature for our 6 Optode floats based on only the measurements below 200 dbar. Assuming an upward velocity of the float of 0.09 dbar/sec (e.g., Johnson et al., 2007), one can infer an equilibration time of the Optode temperature sensor of about 27-33 seconds. This confirms the earlier finding that the slow equilibration of the Optode temperature sensor is a major reason for some of the Optode biases. Recognizing this, Körtzinger et al. (2005) suggested that more accurate oxygen values can be obtained by recalculating the oxygen concentration using the CTD-based temperature measurement.

Figure A3.3 also shows the improvement that can be obtained by replacing the temperature measurements. In the permanent thermocline the differences are now reduced to about 0.5-1 μ-mol kg^{-1}, and even in the seasonal thermocline the differences are below 3 μ-mol kg^{-1}.This is a very substantial improvement, particularly when considering that the larger differences in the seasonal thermocline may reflect real differences arising from the spatial and temporal separation of the measurements.

This recalculation of the oxygen concentration needs the full-set of sensor calibration parameters of the float in addition to the temperature data obtained by the Optode. However, only a few Optode floats contain information onsensor calibration parameters in their

metadata files, which means that this re-calculation (improvement) of oxygen data can presently be done only by the PIs who deployed the floats. Some of the recent APEX/ARGOS/Optode floats do not send Optode temperature because of the reduction of amount of float data (Gilbert, personal communication). Thus, it might be advantageous that the data transmitted from APEX/ARGOS/Optode floats and associated with the oxygen measurement send the raw measurements rather than computed data.

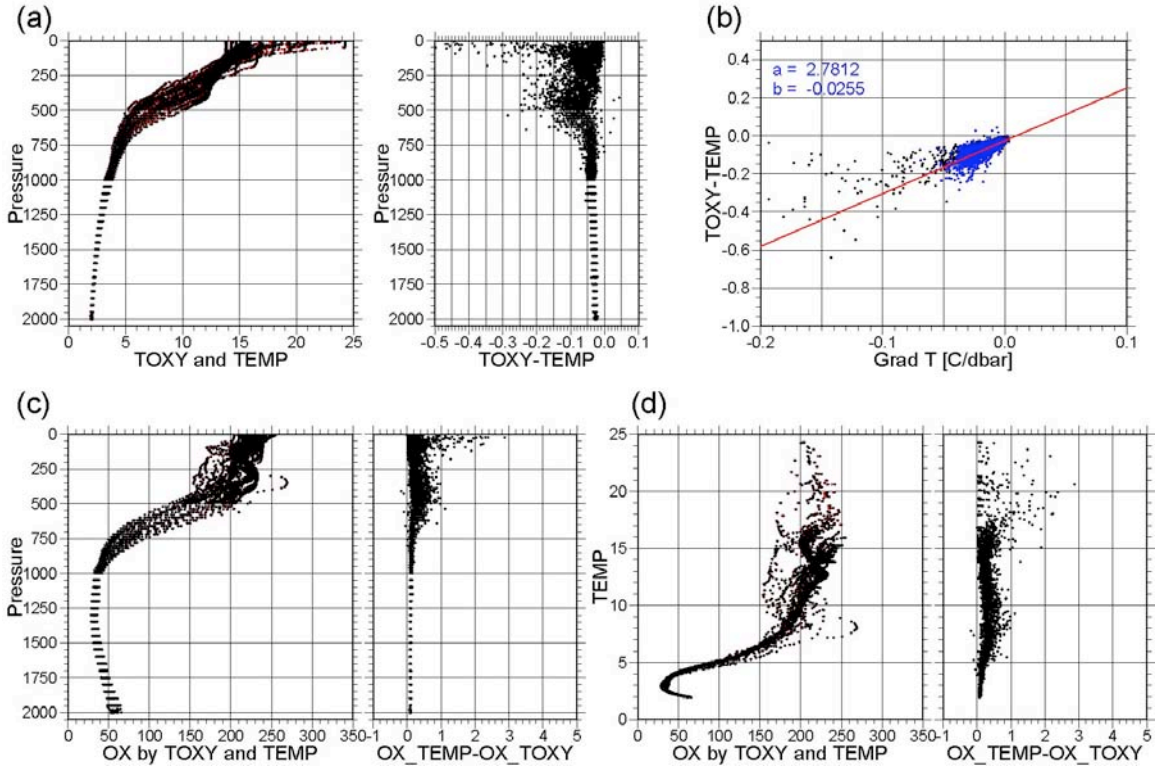

Figure A3.3: Improvement of Optode oxygen by replacement of temperature data for WMO 2900542 (the cyan float in Figure A3.2). (a) In situ temperature by CTD (T_{CTD}, black) and Optode (T_{DO}, red) and their difference ($T_{DO} - T_{CTD}$), (b) relation between their difference and vertical gradient of temperature (T_{CTD}) [C°/dbar], (c, d) Oxygen data of raw (with T_{DO}, red)I and improved (with T_{CTD}, black) and their differences (Improved – Raw, unit is [_-mol kg^{-1}]) with the vertical axis of (c) pressure and (d) in situ temperature. The blue data in (b) represent the measurements at the depth deeper than 200 dbar, which give the regression line (red).

8.4 Results on long-term drift stability from Labrador Sea, tropical Atlantic and Weddell Sea (from Arne Körtzinger)

During recent year we deployed several APEX oxygen floats in the Labrador/Irminger Sea (2003: 2 floats, 2004: 4 floats with additional RAFOS option), tropical Atlantic Ocean (2004: 3 floats, 2006: 3 floats), and Weddell Sea/South Atlantic (2005: 3 floats, 2006: 3 floats; all with additional ice detection algorithm and RAFOS option). Shown below are results from those floats which were operational for at least 1.5 years. Data are raw oxygen readings (and calculated neutral densities) at depths of typically 1800 dbar, where no temporal variability and generally small lateral gradient are expected. Oxygen changes in these time-series are usually accompanied by changes in neutral density indicating that the isobaths are intersecting density layers and hence changing water masses. Often these changes in oxygen and density are seen when the trajectories show rapid translation and relocation into other ocean regions/basins. The data show no sign of typical sensor drift, i.e. change in oxygen readings with time in a consistent direction.

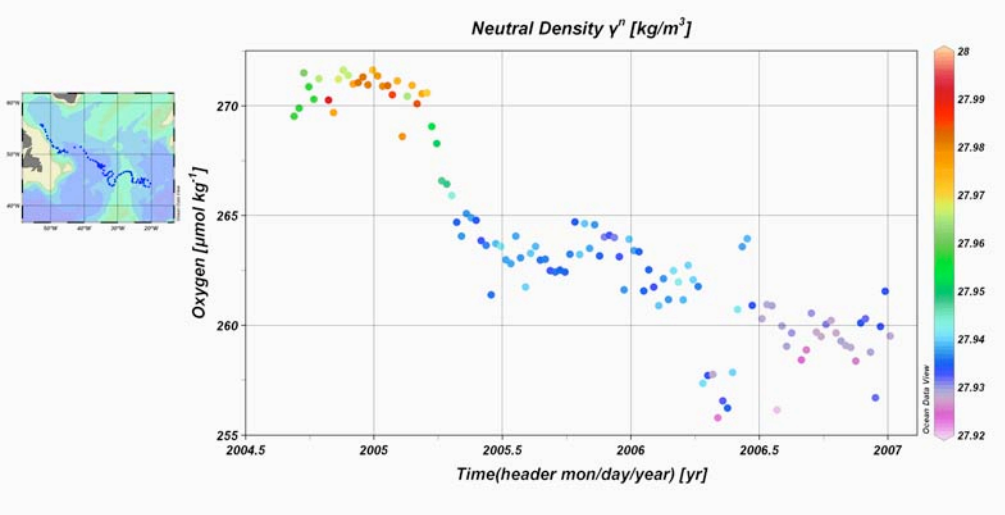

Fig. A4.1: Time-series of oxygen and neutral density at 1800 dbar from WMO float 4900608.

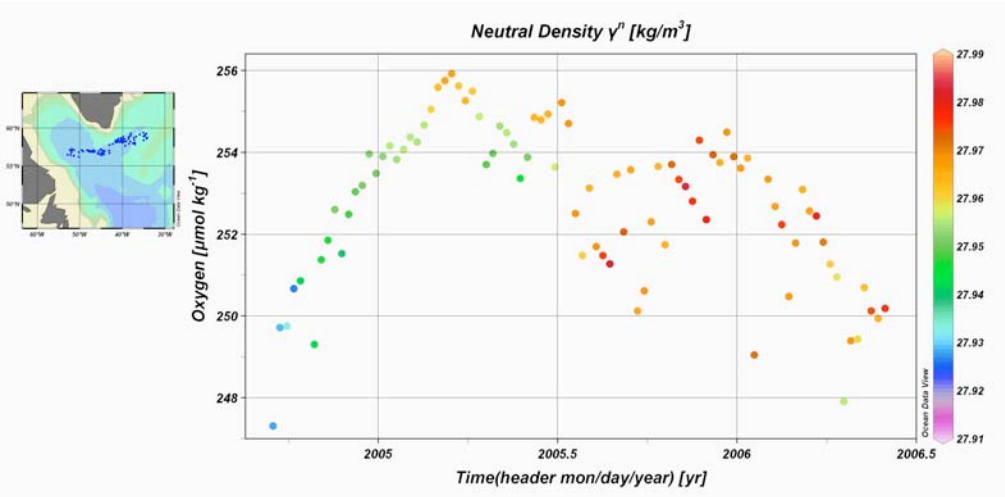

Fig. A4.2: Time-series of oxygen and neutral density at 1800 dbar from WMO float 4900609.

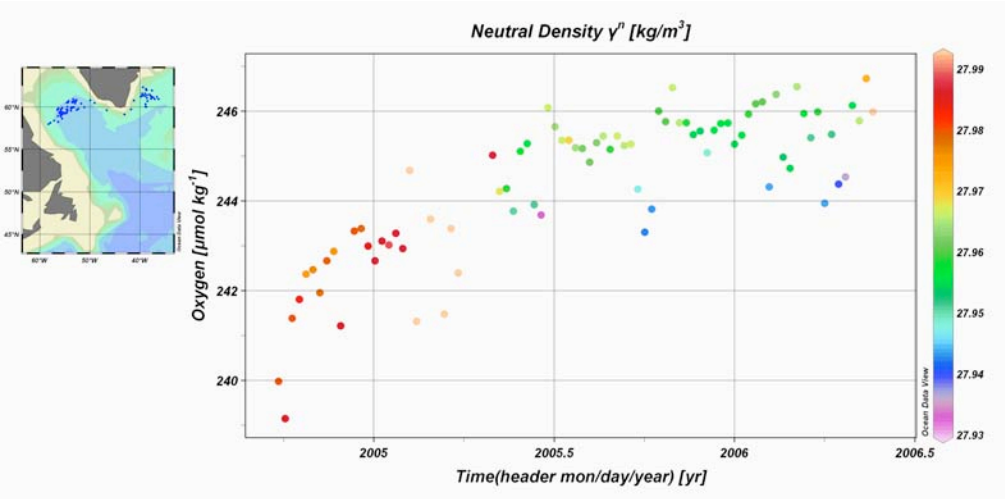

Fig. A4.3: Time-series of oxygen and neutral density at 1800 dbar from WMO float 4900610.

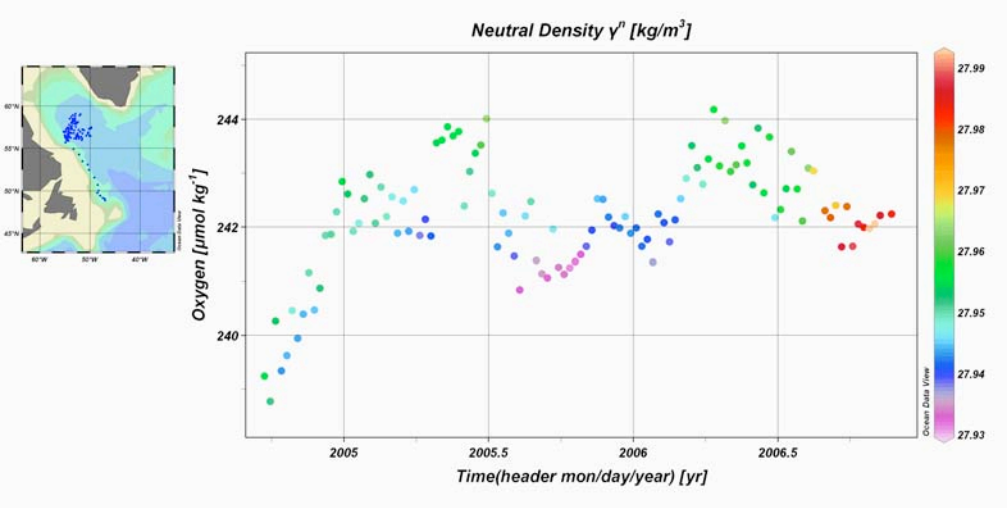

Fig. A4.4: Time-series of oxygen and neutral density at 1800 dbar from WMO float 4900611.

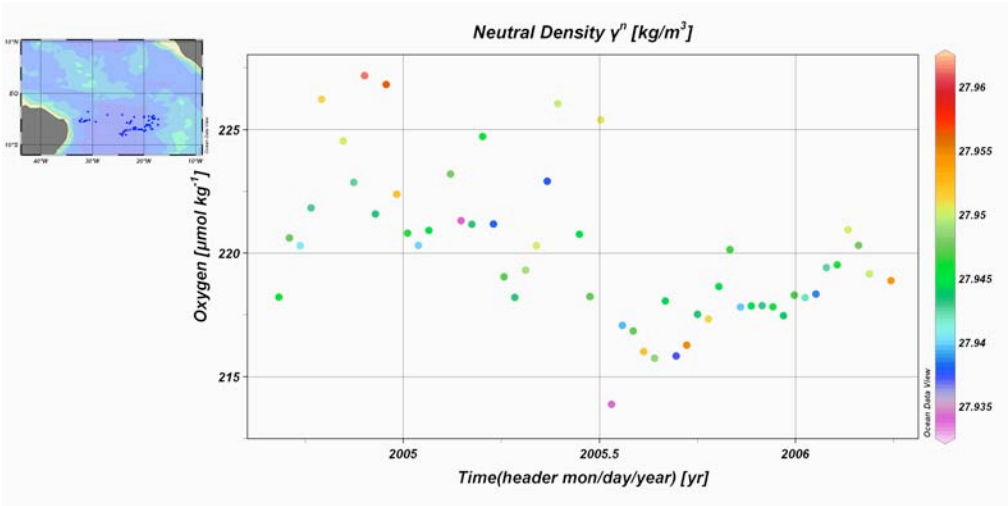

Fig. A4.5: Time-series of oxygen and neutral density at 1800 dbar from WMO float 3900274.

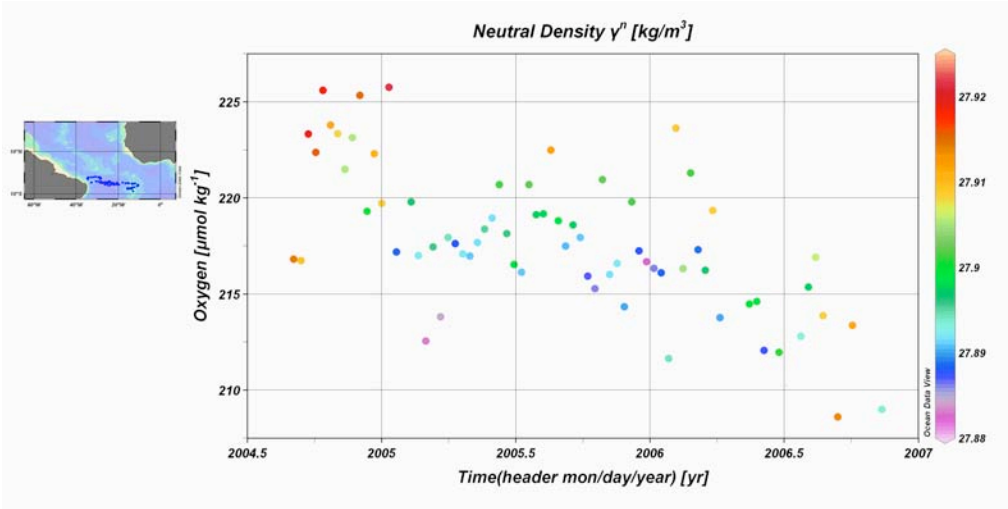

Fig. A4.6: Time-series of oxygen and neutral density at 1600 dbar from WMO float 3900275.

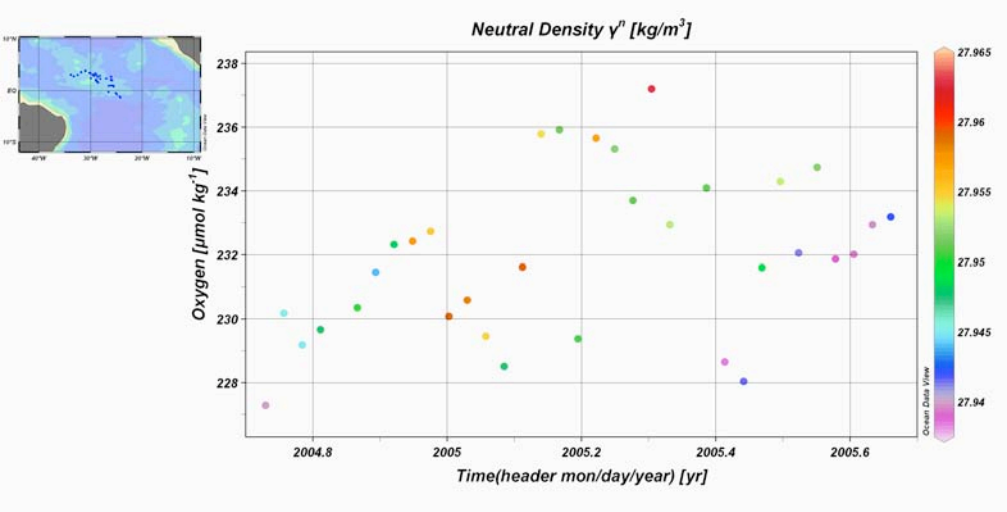

Fig. A4.7: Time-series of oxygen and neutral density at 1800 dbar from WMO float 3900281.

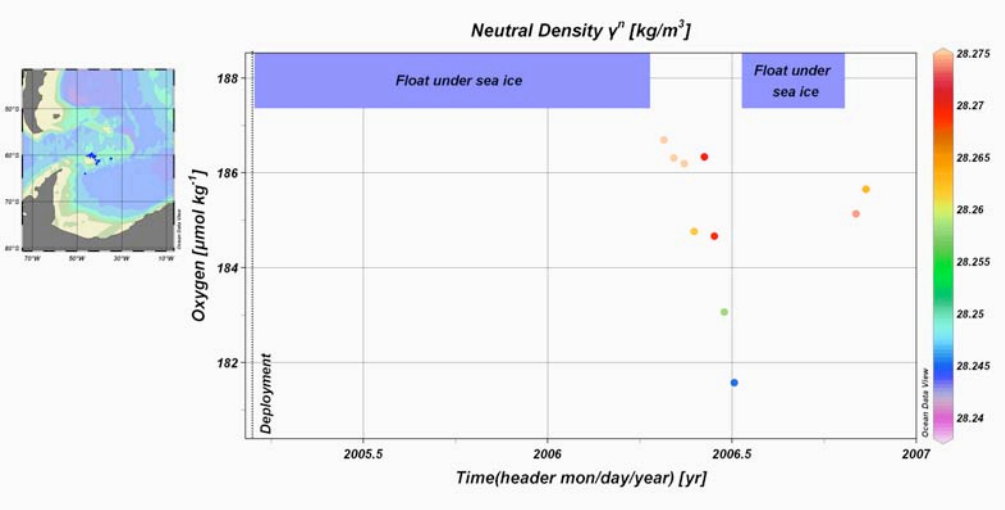

Fig. A4.8: Time-series of oxygen and neutral density at 1800 dbar from WMO float 7900095.

8.5 Currently deployed Argo floats with oxygen sensors

Table A5.1 shows a list of the Argo floats that have reported near real-time oxygen data between December 1, 2006 and January 8, 2007. It shows the already quite broad use of this technology, with many PIs in many countries participating.

Table A5.1: Summary of currently active Argo floats with oxygen sensors (as of January 8, 2007)

WMOID	LAT	LONG	YYYY-MM-DD	HH:MM:SS	OCEAN	ARGO-PROGRAM	SCIENTIST
1900650	6.168	-25.852	12/27/06	23:42:00	Atlantic	IFM-GEOMAR	Juergen_FISCHER /Arne KÖRTZINGER
1900651	1.534	-14.381	1/5/07	1:23:00	Atlantic	IFM-GEOMAR	Juergen_FISCHER /Arne KÖRTZINGER
1900652	4.283	-20.231	12/29/06	22:14:59	Atlantic	IFM-GEOMAR	Juergen_FISCHER /Arne KÖRTZINGER
2900460	44.511	-159.289	1/3/07	8:50:29	Pacific	J-ARGO	Toshio_Suga
2900514	43.185	177.336	1/4/07	17:33:04	Pacific	J-ARGO	JAMSTEC
2900540	42.554	171.45	12/26/06	1:21:56	Pacific	J-ARGO	JAMSTEC
2900541	38.646	169.453	1/5/07	6:28:38	Pacific	J-ARGO	JAMSTEC
2900542	33.261	164.277	1/5/07	10:21:50	Pacific	J-ARGO	JAMSTEC
2900616	28.123	140.374	1/1/07	17:00:18	Pacific	J-ARGO	Toshio_Suga
2900765	14.038	89.02	12/2/06	22:06:25	Indian	Indian_Argo	Shailesh_Nayak
3900333	-40.166	-106.6	1/2/07	11:02:24	Pacific	US_ARGO_PROJECT	STEPHEN_RISER
3900334	-36.639	-95.312	1/4/07	20:48:38	Pacific	US_ARGO_PROJECT	STEPHEN_RISER
3900344	-36.062	-116.636	1/2/07	14:23:02	Pacific	US_ARGO_PROJECT	STEPHEN_RISER
3900345	-38.725	-106.678	1/4/07	20:47:59	Pacific	US_ARGO_PROJECT	STEPHEN_RISER
3900346	-38.388	-94.34	1/7/07	2:46:38	Pacific	US_ARGO_PROJECT	STEPHEN_RISER
3900347	-34.504	-80.171	12/31/06	16:16:12	Pacific	US_ARGO_PROJECT	STEPHEN_RISER
3900348	-37.201	-88.69	1/1/07	20:19:15	Pacific	US_ARGO_PROJECT	STEPHEN_RISER
3900515	-16.852	-77.742	12/31/06	9:47:00	Pacific	ARGO_CHILE	Dr_Osvaldo_ULLOA
3900516	-13.321	-83.865	1/4/07	8:21:59	Pacific	ARGO_CHILE	Dr_Osvaldo_ULLOA
3900521	-22.863	-71.998	1/2/07	9:54:59	Pacific	ARGO_CHILE	Dr_Osvaldo_ULLOA
3900522	-22.608	-80.027	1/1/07	9:47:00	Pacific	ARGO_CHILE	Dr_Osvaldo_ULLOA
3900523	-19.196	-76.876	12/31/06	9:47:59	Pacific	ARGO_CHILE	Dr_Osvaldo_ULLOA
3900524	-16.093	-80.111	12/30/06	9:33:00	Pacific	ARGO_CHILE	Dr_Osvaldo_ULLOA
4900345	49.367	-39.567	1/3/07	2:35:51	Atlantic	US_ARGO_PROJECT	STEPHEN_RISER
4900494	54.882	-47.419	12/31/06	12:02:00	Atlantic	Canadian_Argo	HFreeland_DGilbert
4900497	34.97	-67.948	12/27/06	15:56:00	Atlantic	Canadian_Argo	HFreeland_DGilbert
4900523	51.243	-149.909	1/4/07	4:27:00	Pacific	Canadian_Argo	HFreeland_DGilbert
4900608	44.952	-22.213	1/4/07	11:06:00	Atlantic	ARGO EQ. IFM2	Arne KÖRTZINGER

4900627	32.732	-60.622	1/5/07	0:29:00	Atlantic	Canadian_Argo	HFreeland_DGilbert
4900637	46.348	-128.096	1/4/07	12:06:59	Pacific	Canadian_Argo	HFreeland_DGilbert
4900651	38.918	-164.434	1/1/07	13:23:24	Pacific	J-ARGO	kensuke_Takeuchi
4900652	36.505	-167.174	1/2/07	11:01:53	Pacific	J-ARGO	kensuke_Takeuchi
4900869	53.356	-142.599	1/1/07	12:40:59	Pacific	Canadian_Argo	HFreeland_DGilbert
4900870	56.987	-141.028	1/3/07	1:47:00	Pacific	Canadian_Argo	HFreeland_DGilbert
4900871	49.325	-145.132	1/4/07	2:48:00	Pacific	Canadian_Argo	HFreeland_DGilbert
4900872	50.129	-136.21	1/4/07	23:01:59	Pacific	Canadian_Argo	HFreeland_DGilbert
4900873	38.765	-144.133	1/1/07	2:03:00	Pacific	Canadian_Argo	HFreeland_DGilbert
4900874	43.287	-138.254	1/2/07	4:43:59	Pacific	Canadian_Argo	HFreeland_DGilbert
4900879	54.455	-52.052	12/27/06	4:23:00	Atlantic	Canadian_Argo	HFreeland_DGilbert
4900880	61.248	-59.66	1/5/07	7:52:59	Atlantic	Canadian_Argo	HFreeland_DGilbert
4900881	41.987	-64.289	12/30/06	19:57:00	Atlantic	Canadian_Argo	HFreeland_DGilbert
4900882	43.283	-57.632	1/3/07	14:42:59	Atlantic	Canadian_Argo	HFreeland_DGilbert
4900883	44.026	-53.374	12/28/06	11:39:59	Atlantic	Canadian_Argo	HFreeland_DGilbert
4900905	35.518	-163.836	1/5/07	21:46:49	Pacific	J-ARGO	Toshio_Suga
5900841	-42.801	131.768	12/26/06	21:22:40	Indian	Argo_AUSTRALIA	Susan_Wijffels
5900952	23.188	-160.32	1/5/07	10:04:00	Pacific	US_ARGO_PROJECT	STEPHEN_RISER
5900961	55.265	-138.004	1/7/07	6:10:39	Pacific	US_ARGO_PROJECT	STEPHEN_RISER
5900965	-45.529	-166.253	1/6/07	15:08:20	Pacific	US_ARGO_PROJECT	STEPHEN_RISER
5900966	-51.382	-137.775	12/31/06	18:02:59	Pacific	US_ARGO_PROJECT	STEPHEN_RISER
5901042	-40.881	-174.464	12/31/06	2:45:53	Pacific	US_ARGO_PROJECT	STEPHEN_RISER
5901043	-40.99	-159.973	1/1/07	22:46:10	Pacific	US_ARGO_PROJECT	STEPHEN_RISER
5901044	-43.664	-161.563	1/2/07	13:33:18	Pacific	US_ARGO_PROJECT	STEPHEN_RISER
5901045	-41.623	-161.028	1/1/07	0:52:55	Pacific	US_ARGO_PROJECT	STEPHEN_RISER
5901046	-47.416	-155.994	1/1/07	17:10:53	Pacific	US_ARGO_PROJECT	STEPHEN_RISER
5901047	-43.275	-156.561	1/3/07	12:01:42	Pacific	US_ARGO_PROJECT	STEPHEN_RISER
5901048	-44.034	-143.88	1/4/07	14:09:42	Pacific	US_ARGO_PROJECT	STEPHEN_RISER
5901049	-40.331	-145.419	1/2/07	22:51:22	Pacific	US_ARGO_PROJECT	STEPHEN_RISER
5901050	-42.964	-141.932	1/5/07	13:19:56	Pacific	US_ARGO_PROJECT	STEPHEN_RISER
5901051	-44.676	-148.691	1/3/07	14:35:32	Pacific	US_ARGO_PROJECT	STEPHEN_RISER
5901052	-38.794	-143.823	1/5/07	5:13:10	Pacific	US_ARGO_PROJECT	STEPHEN_RISER
5901053	-39.439	-131.885	12/31/06	3:50:51	Pacific	US_ARGO_PROJECT	STEPHEN_RISER

5901054	-37.567	-121.532	12/31/06	6:12:10	Pacific	US_ARGO_PROJECT	STEPHEN_RISER
5901069	25.504	-164.007	1/6/07	16:51:07	Pacific	US_ARGO_PROJECT	STEPHEN_RISER
5901165	-50.911	143.564	12/31/06	22:51:45	Indian	Argo_AUSTRALIA	Susan_Wijffels
5901178	-53.287	110.805	12/26/06	10:00:23	Indian	Argo_AUSTRALIA	Susan_Wijffels
5901336	18.611	-152.987	12/31/06	12:57:03	Pacific	US_ARGO_PROJECT	STEPHEN_RISER
5901338	15.269	-153.826	1/1/07	16:12:00	Pacific	US_ARGO_PROJECT	STEPHEN_RISER
5901339	12.091	-151.448	1/2/07	0:00:17	Pacific	US_ARGO_PROJECT	STEPHEN_RISER
6900346	60.629	-25.488	12/29/06	5:39:59	Atlantic	WEN	Detlef_QUADFASEL
6900347	67.557	-1.578	12/29/06	0:29:59	Atlantic	WEN	Detlef_QUADFASEL
6900499	68.485	-1.154	12/28/06	22:41:59	Atlantic	ARGO_NORWA	Einar_SVENDSEN
6900500	71.692	7.814	12/27/06	22:59:00	Atlantic	ARGO_NORWA	Einar_SVENDSEN
7900095	-60.688	-34.639	12/31/06	22:21:59	Southern Ocean (Atl.)	ARGO_AWI	Olaf_BOEBEL/ Arne KÖRTZINGER
7900132	-63.64	-51.37	12/31/06		Southern Ocean (Atl.)	ARGO_AWI	Olaf_BOEBEL/ Arne KÖRTZINGER
7900133	-58.66	-48.12	01/12/07		Southern Ocean (Atl.)	ARGO_AWI	Olaf_BOEBEL/ Arne KÖRTZINGER
7900134					Southern Ocean (Atl.)	ARGO_AWI	Olaf_BOEBEL/ Arne KÖRTZINGER